Cell Reports

Resource

Dynamics of Chromatin and Transcription during Transient Depletion of the RSC Chromatin Remodeling Complex

Graphical Abstract

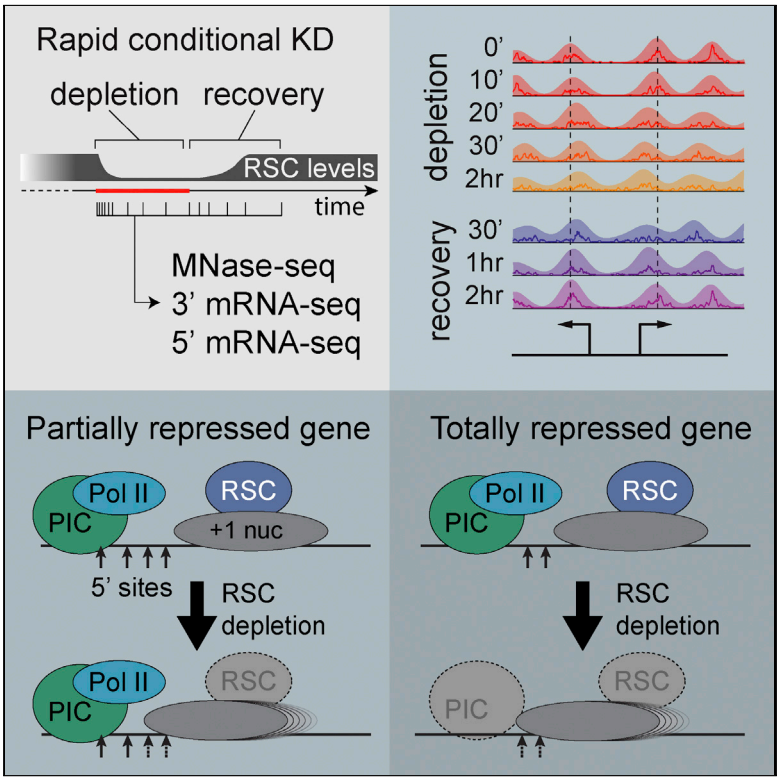

Highlights

- Screen of all yeast ATP-dependent remodelers with a conditional degradation system
- RSC depletion leads to rapid replication-independent NFR fill-in
- Recovery of RSC fully reverses NFR fill-in and transcriptional changes
- RSC-dependent nucleosome positioning directly affect transcription start site choice

Authors

Avital Klein-Brill,
Daphna Joseph-Strauss,
Alon Appleboim, Nir Friedman

Correspondence

nir.friedman@mail.huji.ac.il

In Brief

Klein-Brill et al. track changes in nucleosome positioning at a detailed time course during rapid depletion and re-introduction of RSC, an essential ATP-dependent chromatin remodeler. Measuring changes in mRNA transcripts structure and levels they dissect how shifts in nucleosome positions affect choice of exact transcription start site.

Klein-Brill et al., 2019, Cell Reports *26*, 279–292
January 2, 2019
https://doi.org/10.1016/j.celrep.2018.12.020

CellPress

Cell Reports
Resource

Dynamics of Chromatin and Transcription during Transient Depletion of the RSC Chromatin Remodeling Complex

Avital Klein-Brill,[1] Daphna Joseph-Strauss,[1] Alon Appleboim,[1] and Nir Friedman[1,2,*]
[1]School of Engineering and Institute of Life Sciences, The Hebrew University of Jerusalem, Jerusalem 9190401, Israel
[2]Lead Contact
*Correspondence: nir.friedman@mail.huji.ac.il
https://doi.org/10.1016/j.celrep.2018.12.020

SUMMARY

Nucleosome organization has a key role in transcriptional regulation, yet the precise mechanisms establishing nucleosome locations and their effect on transcription are unclear. Here, we use an induced degradation system to screen all yeast ATP-dependent chromatin remodelers. We characterize how rapid clearance of the remodeler affects nucleosome locations. Specifically, depletion of Sth1, the catalytic subunit of the RSC (remodel the structure of chromatin) complex, leads to rapid fill-in of nucleosome-free regions at gene promoters. These changes are reversible upon reintroduction of Sth1 and do not depend on DNA replication. RSC-dependent nucleosome positioning is pivotal in maintaining promoters of lowly expressed genes free from nucleosomes. In contrast, we observe that upon acute stress, the RSC is not necessary for the transcriptional response. Moreover, RSC-dependent nucleosome positions are tightly related to usage of specific transcription start sites. Our results suggest organizational principles that determine nucleosome positions with and without RSC and how these interact with the transcriptional process.

INTRODUCTION

Nucleosomes form the basic repeating unit of DNA packaging in eukaryotic cells. Each consists of a ~147-bp double-stranded DNA wrapped around an octamer of histone proteins and separated by a short linker DNA (Kornberg, 1974). Nucleosomes restrict DNA accessibility (Bell et al., 2011), and their precise position relative to the underlying DNA sequence affects virtually all DNA-templated processes, including DNA repair (Bucceri et al., 2006), DNA replication (Méchali, 2010), and transcription (Workman, 2006). Therefore, nucleosome positioning over the genome has an important regulatory role.

Global mapping of nucleosome positioning have revealed a stereotypical arrangement of nucleosomes at genes, with a nucleosome-depleted region (NDR) or nucleosome-free region (NFR) at the promoters of genes followed by a well-positioned nucleosome at the +1 position (immediately downstream of the NFR). This +1 nucleosome is positioned at a relatively fixed distance from the transcription start site (TSS) and the positioning of the pre-initiation complex. The +1 nucleosome is followed by an array of constant-spaced nucleosomes through the gene body. The end of a gene is often also marked with an NDR downstream of the transcription termination site (TTS) (Jiang and Pugh, 2009a; Lee et al., 2007; Rhee and Pugh, 2012; Yuan et al., 2005).

The pattern of nucleosome positioning through the genome is determined by multiple *cis*- and *trans*-acting factors. Intrinsic properties of DNA sequences contribute mainly to the depletion of nucleosomes at NFRs, together with chromatin remodeling complexes and general regulatory factors (GRFs; ABF1, REB1, and RAP1). Furthermore, the position of nucleosomes is affected by ATP-dependent processes, including the transcription machinery and ATP-dependent chromatin remodelers (Hughes et al., 2012; Lee et al., 2007; Ozonov and van Nimwegen, 2013; Yuan et al., 2005; Zhang et al., 2011b).

Chromatin remodelers are conserved multisubunit complexes that utilize ATP hydrolysis to disrupt DNA-histone contacts to restructure, slide, or evict nucleosomes (Clapier and Cairns, 2009). There are few classes of chromatin remodelers (SWI/SNF, ISWI, INO80, SWR1, and CHD) that are all conserved from yeast to humans. Chromatin remodelers are implicated in establishing NFRs and positioning of NFR-adjacent nucleosomes (Clapier and Cairns, 2009; Krietenstein et al., 2016).

RSC (remodel the structure of chromatin) is an abundant and essential nuclear protein complex that is homologous to the SWI/SNF chromatin remodeler complex (Cairns et al., 1996). RSC has a role in transcription initiation and elongation (Floer et al., 2010; Hartley and Madhani, 2009; Parnell et al., 2008; Spain et al., 2014) and is important for additional processes in the cell, including chromosome replication, segregation, and repair (Chai et al., 2005; Hsu et al., 2003). *In vitro*, RSC can either disassemble or slide nucleosomes along a DNA sequence (Chaban et al., 2008; Lorch et al., 1999; Montel et al., 2011). AT-rich DNA sequences facilitate RSC activity, and incubation of purified chromatin with RSC leads to selective removal of promoter nucleosomes in a sequence-dependent manner (Krietenstein et al., 2016; Lorch et al., 2011). *In vivo*, RSC depletion leads to global movement of nucleosomes toward the NFR (Ganguli et al., 2014; Hartley and Madhani, 2009; Kubik et al., 2018; Parnell et al., 2008, 2015). RSC and GRFs are both required for NFR formation of some genes, while NFR formation of other genes require RSC, but not GRF binding (Hartley and Madhani, 2009; Kubik et al., 2018).

RSC activity in establishing NFRs has functional implications on transcription. *In vitro*, the initiation of transcription is repressed by a nucleosome placed on the TSS (Lorch et al., 1987). *In vivo*, many studies on a small set of genes have shown that nucleosome depletion leads to gene activation (Han and Grunstein, 1988; Lohr, 1997). Overall, gene expression is correlated with nucleosome depletion in the promoter both at steady state and during environmental changes. However, open NFRs are found also in genes that are rarely transcribed, and chromatin reorganization is not always linked to changes in transcription (Gkikopoulos et al., 2011; Lee et al., 2007; Shivaswamy et al., 2008; Zhang et al., 2011a). Recent study suggested that in RSC-depleted cells the shift in nucleosome position decreases TATA-binding protein (TBP) binding, thus inhibiting transcription (Kubik et al., 2018). However, little correlation was found between NFR filling and transcription inhibition in RSC-depleted cells (Ganguli et al., 2014; Hartley and Madhani, 2009). In addition, it was claimed that RSC might be recruited by the transcriptional machinery upon induction to induce gene expression through chromatin remodeling (Damelin et al., 2002; Mas et al., 2009; Ng et al., 2002).

While RSC has been extensively studied, there are pertinent questions that are still unanswered, mainly due to limitations of experimental tools: (1) RSC depletion has been shown to cause mis-segregation defects (Hsu et al., 2003). Do these defects represent a separate role for RSC, or are they a consequences of its role in transcription? Moreover, the replication of chromosome involves major disruption of the nucleosome template, raising the question whether RSC depletion effects are due to its function during and after S phase. (2) RSC is essential, indicating fatal failures without its activity. Nonetheless, to what extent can cells recover proper chromatin template after a transient depletion of RSC during which most NFRs are disrupted? (3) What are the timescales of RSC activity? Is it needed reorganize the chromatin template once per cell cycle, or is constantly active in maintaining the organization of the template? Almost all studies of RSC depletion examined chromatin at 1 hr or later after the depletion and cannot determine shorter timescales. (4) What are the timescales of the effect of depletion on transcription? Is this a direct and immediate effect? (5) Is RSC needed during transcription initiation, or is it required mostly to establish the NFRs prior to initiation? (6) Can we understand how specifically RSC-dependent nucleosome positioning affects transcription initiation and transcript structure? Is disruption in polymerase initiation complex (PIC) assembly (Kubik et al., 2018) the only mechanism?

Answering such questions about RSC and other chromatin remodelers *in vivo* is challenging for several reasons. As with all chromatin-related factors, remodeler action is potentially pervasive throughout the genome and can have dramatic global consequences. Chromatin remodelers are involved in many cellular processes, and therefore it is difficult to distinguish their direct and indirect effects. Moreover, some of the ATPase units of chromatin remodelers are essential. Indeed, previous works on RSC used a variety of perturbations, including deletion of inessential subunits, such as Rsc8 (Ganguli et al., 2014), temperature-sensitive alleles of Sth1 (Hartley and Madhani, 2009; Parnell et al., 2008, 2015), anchor-away tagging of Sth1 (Kubik et al., 2018), which induce irreversible removal of the Sth1 from the nucleus, and auxin-mediated degradation of Sth1 (Parnell et al., 2015), which we expand on below.

Here, we study the role of chromatin remodeling proteins on nucleosome organization and transcription using their conditional degradation. We implemented the auxin (indole-3-acetic acid [IAA])-inducible degradation system that allows for rapid and reversible degradation of proteins (Morawska and Ulrich, 2013; Nishimura et al., 2009). Unlike earlier knockdown systems studying chromatin remodeler activity, the auxin-inducible system involves little perturbation to the cells and allows recovery. We follow the dramatic change in NFR structure following RSC depletion and recovery at a high temporal resolution and study the interaction between replication, transcription, and chromatin dynamics in RSC-depleted cells. Finally, based on our observations, we propose simple model explaining the transcriptional inhibition following RSC depletion.

RESULTS

Conditional Knockdown System for Studying Chromatin Remodelers

Studying the function of ATP-dependent chromatin remodelers is complicated by their central role in chromatin biology. Some, such as Sth1 (RSC), are essential and cannot be deleted, while others can be deleted (Gkikopoulos et al., 2011; Ocampo et al., 2016; Tirosh et al., 2010; Whitehouse et al., 2007), but the resulting chromatin structure potentially reflects accumulated contribution over multiple cell divisions and various other pleiotropic effects. To better understand the direct roles of remodelers, we sought to use a quick-acting conditional knockout system.

We implemented the auxin-inducible degron (AID) system (Morawska and Ulrich, 2013), yielding an auxin-inducible, rapid degradation of tagged chromatin remodelers (Figure 1A). We constructed AID-tagged version of the major ATP-dependent remodelers: Chd1, Fun30, Ino80, Isw1 (ISW1A and ISW1B complexes), Isw2, Snf2 (the SWI/SNF complex), Sth1 (the catalytic unit of the RSC complex), and Swr1. All strains were viable when grown without auxin, exhibiting normal growth rates (data not shown). In all eight strains, western blot analysis showed drastic reduction of degron-tagged proteins after introduction of auxin (Figure S1A). We also considered that the addition of the tag might itself perturb protein function or premature auxin-independent degradation. However, in all eight strains, nucleosome positions in the absence of auxin as measured by MNase-seq (STAR Methods; Figures 1B and S1B) were virtually identical to nucleosome positions in the ancestral untagged strain.

Comparing nucleosome positions before and after auxin addition (Figure 1B) in the different strains showed a range of effects; degradation of either Ino80 or Sth1 lead to dramatic changes in nucleosome positioning, while degradation of Fun30 and Snf2 had little or no effect. Overall, we expected the chromatin structure following degradation to converge in time to the structure of the deletion strains, when these are viable. We constructed fresh deletion strains of the nonessential remodelers to assay

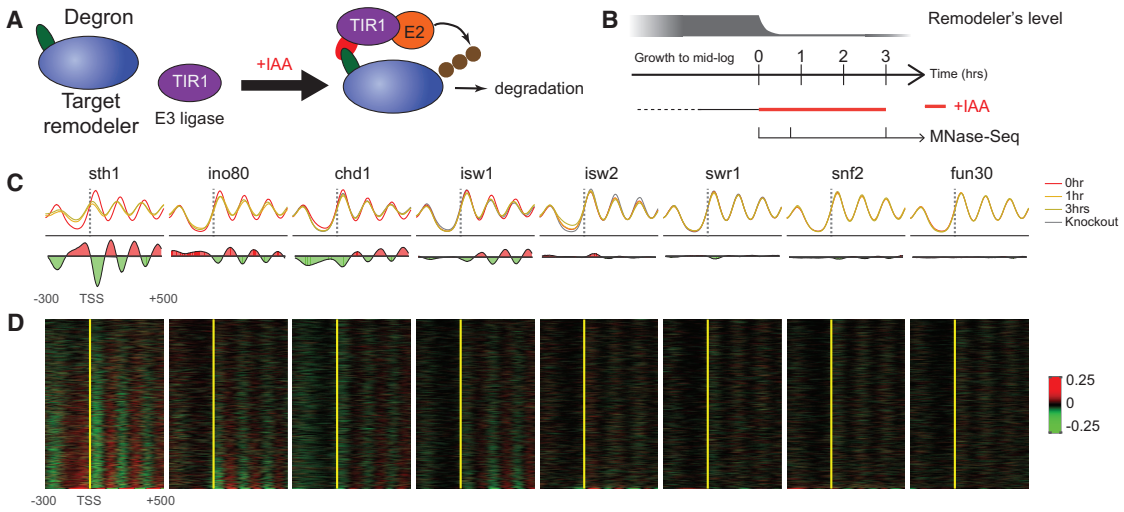

Figure 1. Induced Knockdown Screen of ATP-Dependent Chromatin Remodelers

(A) An auxin-inducible degron (AID) system (Morawska and Ulrich, 2013) yielding an auxin-inducible, rapid degradation of tagged chromatin remodelers. Plant hormone auxin (IAA) directly induces rapid degradation of the AID-tagged protein by mediating the interaction of a degron domain in the target protein with the substrate recognition domain of TIR1.

(B) Experimental outline. AID-tagged chromatin remodeler strains were grown to mid-log in YPD. MNase-seq was performed to compare nucleosome positioning before and at two time points after auxin addition.

(C) Average MNase coverage positioned relative to the transcription start site (TSS) ("metagene") for each chromatin remodeler AID strain before and after auxin addition and in the relevant KO strains (if available) (top). Average of the change in MNase coverage before and after auxin addition (1 hr to 0 hr) positioned relative to the TSS for each chromatin remodeler AID strain (bottom).

(D) Heatmaps representing the change in MNase coverage before and after auxin addition (1 hr to 0 hr) positioned relative to the TSS (in yellow) for each AID strain. Genes (rows) are sorted, in each strain, by the magnitude of changes in coverage following the depletion in the NFR area.

See also Figure S1.

nucleosome positions. We failed in multiple attempts to construct deletion strains of Snf2 and Ino80, as these were either inviable or displayed sluggish growth. Of the remaining four deletion strains (chd1Δ, isw1Δ, isw2Δ, and swr1Δ), we could compare the deletion strain to 3 hr depletion. In Chd1 depletion, we saw similar effects to these seen in a deletion strain, with most of the changes in nucleosome positioning along gene bodies (Figures 1C, 1D, and S1C). In fact, these changes were mostly established after 1 hr, suggesting that Chd1 is constantly active in nucleosome positioning, in agreement with its known role in transcription (Simic et al., 2003). Consistent with prior reports (Tirosh et al., 2010; Whitehouse et al., 2007; Yen et al., 2012), both isw1Δ and Isw1 depletion displayed upstream shift in +1 and gene body nucleosomes, and both isw2Δ and Isw2 depletion displayed a mild increase in NFR size (Figures 1C, 1D, and S1C). Swr1 deletion and depletion had little effect on nucleosome positions.

Examining all eight depletion strains, two strains stood out as having a strong effect on nucleosome positioning (Figures 1C and 1D). Sth1-depletion resulted in a noticeable shift in +1 and −1 nucleosomes into the NFR in many genes. This trend is consistent with prior reports using other conditional perturbations (Ganguli et al., 2014; Hartley and Madhani, 2009; Kubik et al., 2018; Parnell et al., 2008). Consistent with prior reports (Yao et al., 2016; Yen et al., 2012), depletion of Ino80 led to mild increase in NFR size and increased the fuzziness of nucleosomes throughout the gene (Figure S1D). In both cases, the effect we observe *in vivo* is consistent with a recent genome-wide *in vitro* reconstitution study (Krietenstein et al., 2016). These results further demonstrate the utility of conditional knockdown for studying remodeler function directly.

Massive Disruption of Chromatin Structure following Sth1 Depletion

Given the dramatic effect of Sth1 depletion on promoter nucleosome architecture, we decided to further explore its function. The rapid degradation system allowed us to monitor nucleosome dynamics through RSC depletion at a fine temporal resolution. Auxin was added to exponentially growing cells, which were subsequently crosslinked at various time points and subjected to MNase-seq (Figure 2A).

The most evident effect of Sth1 depletion is a gradual and global shift in nucleosome positioning into the NFR, to which we will refer as "NFR fill-in." In general, we observe the −1 and +1 nucleosomes shifting into the NFR with coordinated move of their flanking template (Figure 2B). This change is accompanied by increased "fuzziness" in nucleosome positions (Figures 2B, 2C, and S2C). However, there are few exceptions, including the GAL1-GAL10 promoter, where the fill-in is manifested by a new nucleosome in the NFR, with little or no shift in +1 and/or −1 nucleosomes (Figure S2D) (Ramachandran et al., 2015).

NFR widths in growing yeast present a bimodal distribution (Figure 2D). Genes with short ("closed") NFRs (150–200 bp;

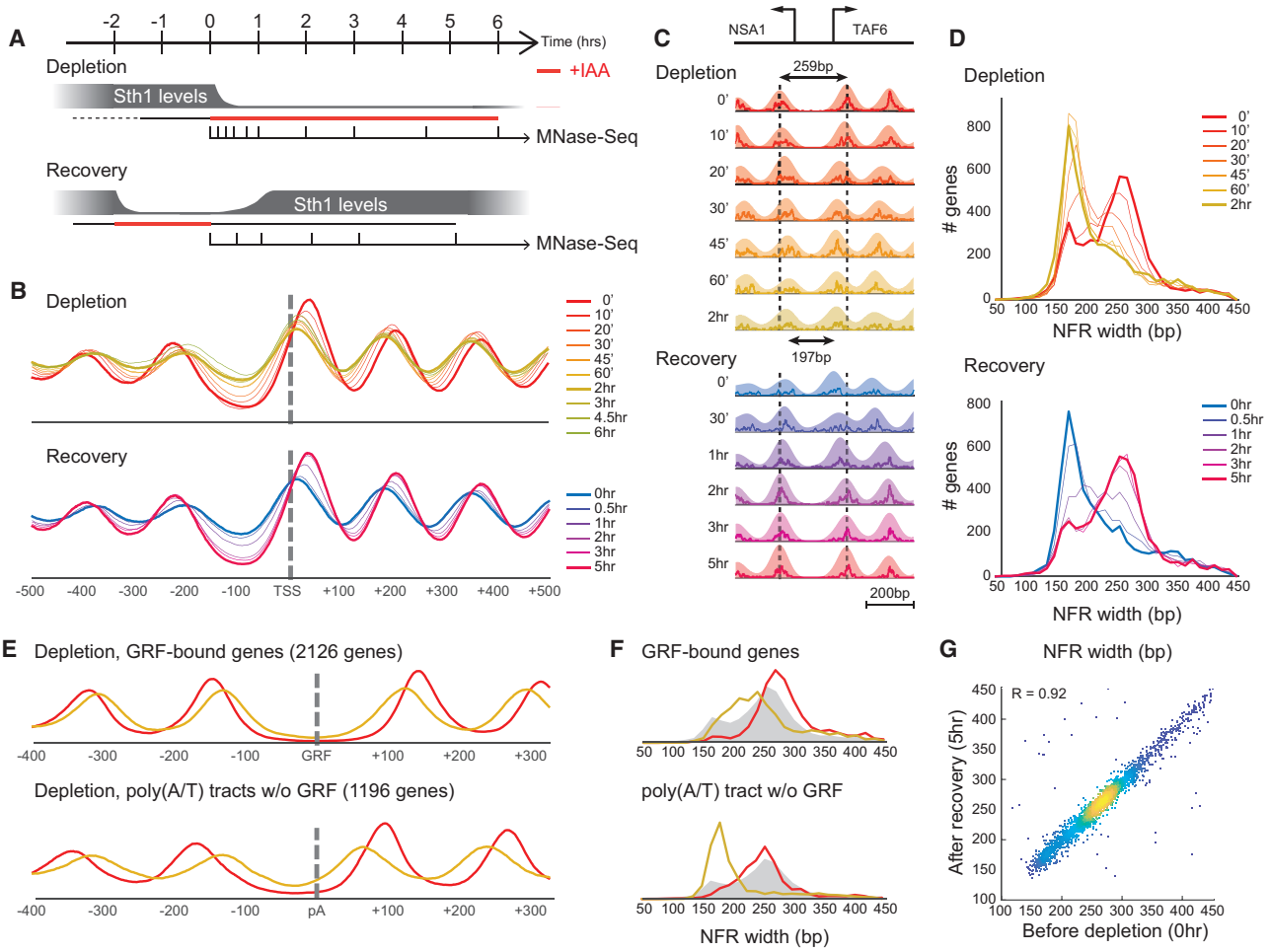

Figure 2. Dynamics of Sth1 Depletion and Recovery Show Massive yet Reversible Disruptions in Chromatin Organization

(A) Experimental outline. For depletion, auxin (IAA) was added to mid-log degron-Sth1 cells, and MNase-seq was performed at the indicated time points. For recovery, mid-log degron-Sth1 cells were incubated in the presence of auxin for 2 hr. Auxin was washed from the media, and MNase-seq was performed at the indicated time points.

(B) Median MNase coverage positioned relative to the TSS (metagene) following Sth1 depletion (top) and recovery (bottom).

(C) MNase read centers (lines, dark color) and coverage (shade, light color) following Sth1 depletion and recovery in the TAF6/NSA1 promoter area. Dashed lines represent the position of nucleosomes +1 and −1 center before depletion and after full recovery.

(D) Distribution of NFR width (defined as the distance between the peak −/+1 nucleosomes) through sth1 depletion and recovery.

(E) Average MNase coverage (metagene) before (red line) and 1 hr after (yellow line) Sth1 depletion in genes with a GRF-binding site (top) and without GRF binding but with a poly(A/T) tract (bottom). Genes were positioned relative to the GRF-binding site or poly(A/T) tract site. GRF-binding sites were obtained from Gutin et al. (2018).

(F) Distribution of NFR width throughout Sth1 depletion in the two groups as in (E). The distribution of all genes before auxin addition is shown in gray.

(G) Comparison of NFR width before Sth1 depletion and after recovery. Each point is related to NFR of a gene. Genes with fuzzy +1 or −1 nucleosomes were excluded.

See also Figure S2.

Figure 2D) are mostly condition-responsive genes that require chromatin remodeling for activation; in contrast, most constitutively expressed genes have long (“open”) NFRs (250–300 bp) (Field et al., 2008; Rhee and Pugh, 2012; Tirosh and Barkai, 2008). Upon Sth1 depletion, the number of long NFRs shrinks, resulting in a primarily unimodal distribution of NFRs that are mostly short. Strikingly, changes in nucleosome positions were evident within 10–20 min after auxin introduction (Figures 2D and S2B). Within 1 hr, 85% of genes achieved 80% of the maximal NFR change (Figure S2B). The rapidness and extent of change support a direct and crucial role for RSC in maintaining most “open” promoters *in vivo*.

Although most NFRs shrink in response to Sth1 depletion, the extent of the change is variable and the NFR of some genes remains relatively open. Multiple processes are potentially involved in determining NFR width and nucleosome positioning in the absence of RSC. Roughly, one can consider two classes: (1) passive obstacles for nucleosome occupancy, such as bound

transcription factors or unfavorable nucleosome sequences; and (2) active processes, such as transcription-dependent recruitment of other chromatin remodelers. Previous work has shown that in addition to RSC, GRF proteins (Abf1 and Reb1) also have a role in NFR formation (Hartley and Madhani, 2009). It was also shown *in vitro* that AT-rich DNA sequences facilitate RSC's nucleosome removal activity (Krietenstein et al., 2016; Lorch et al., 2014). We find that following RSC depletion, NFRs with GRF-binding sites are maintained with well-positioned nucleosomes flanking the NFR (Figures 2E and 2F), suggesting that GRFs are still present in NFRs and act as a barrier for nucleosomes. In contrast, in promoters that contain poly(A/T) tracts but no GRF-binding site, RSC depletion results in nucleosomes that are fuzzier and generally encroach on the poly(A/T) site, consistent with RSC-dependent expulsion of nucleosomes from poly(A/T) tracts *in vivo* rather than an intrinsic property of poly(A/T) DNA (Figures 2E and 2F).

Chromatin Structure Disruptions Are Fully Reversible upon Sth1 Re-accumulation

The auxin-degron system also allows the conditional recovery of protein levels upon removal of auxin and shutdown of the degradation signal. As was previously shown, upon conditional knockdown of Sth1, most cells were arrested with DNA content characteristic of G2-M stage (Du et al., 1998; Figure S2E) and were viable for 2–3 hr (Parnell et al., 2008) (Figure S2F). Although the chromatin was heavily disrupted after 2 hr, when auxin was removed from the media and Sth1 re-accumulated, cell and growth resumed (Figures 2 and S2F). While this suggests the recovery of chromatin, the degree and rate of chromatin recovery was never studied.

To follow nucleosome dynamics during re-accumulation of Sth1, cells were incubated for 2 hr in the presence of auxin as described earlier, auxin was washed from the media, and cells were resuspended in auxin-free rich media (YPD) (Figure 2A). When Sth1 re-accumulated (Figure S2A), chromatin gradually returned to its state prior to RSC depletion. Surprisingly, full recovery occurred within 2 hr (Figures 2B, 2C, and S2). Overall, the process of recovery was slower than depletion (65% of genes show 40% change after 1 hr), but this can be due the rate of Sth1 synthesis, and/or asynchrony in auxin elimination in the population.

Interestingly, we do not find any evidence of "memory" in chromatin. That is, no locus with well-positioned nucleosomes exhibited a significantly altered chromatin organization after RSC recovery when compared to naive cells (Figure 2G). Since the timescale of the experiment (2 hr) excludes the dilution of RSC-perturbed cells in the growing population, this indicates that nucleosome positioning around the NFR is a highly dynamic process and that a transient perturbation elicits little or no long-term effects to the local chromatin structure.

Sth1-Dependent NFR Clearing Is Replication Independent

The global nature of the changes in chromatin structure in response to Sth1-depletion and re-accumulation suggests the possible involvement of the replication machinery or the possibility of chromatin misassembly in the wake of DNA replication. To investigate whether RSC's main role is reorganization of the chromatin after replication, Sth1-degron cells were arrested in G1 with alpha factor (Figure S3A) and Sth1 degradation was induced by addition of auxin (Figure 3A). The changes in NFR width in arrested cells closely matched the changes we observed during Sth1 depletion in unarrested cells (Figure 3B). To determine if replication is required for reorganizing the chromatin during re-accumulation of RSC, Sth1-depleted cells were washed and resuspended in auxin-free media but in the presence of alpha factor to prevent DNA replication (Figure 3A). We confirmed that these cells did not replicate their DNA (Figure S3B), but nevertheless, the chromatin completely recovered in the arrested cells with kinetics similar to growing cells (Figures 3B and 3C).

These results suggest that RSC is constantly clearing NFRs throughout the cell cycle. Although replication might disrupt nucleosome positions at the NFR, there are additional processes that lead to NFR fill-in even in G1-arrested cells (Parnell et al., 2015). When active, RSC counteracts these processes and maintains open NFR in a DNA-replication-independent manner.

RSC Maintains Open NFRs in Low-Expression Genes

Although there is a clear correlation between NFR width and mid-log transcription levels (Weiner et al., 2010; Yuan et al., 2005), this relationship is not absolute, and there are many poorly expressed genes with an open NFR (Jiang and Pugh, 2009a) (Figure 4C). To further investigate this connection, we performed quantitative RNA sequencing (RNA-seq) in RSC-depleted cells with a reference spike-in of *K. lactis* cells to detect global changes as well as relative changes (Figure 4A; STAR Methods).

It was previously shown that RSC depletion leads to a global inhibition of transcription (Parnell et al., 2008). This global decrease could be either a direct consequence of RSC depletion or an indirect effect due to cellular stress, which eventually leads to cell death. To differentiate between these scenarios, we made detailed time-course measurements of mRNA levels following Sth1 depletion. We found a dramatic reduction in mRNA levels within 30 min after auxin addition, which is ~10–15 min after most cellular Sth1 is depleted (Figure 4B and S4A). The rapid reduction in mRNA levels supports a direct involvement of RSC in maintaining the transcriptional program of the cell. To our surprise, the reduction in mRNA levels was stronger in mid-low-expressed genes (Figures S4A and S4B). A concern with measuring mRNA levels, especially during global transcription inhibition, is that it represents differences in mRNA stability and not synthesis. We used SLAM-seq, a method for metabolic labeling of newly synthesized RNA (Herzog et al., 2017; STAR Methods), to determine whether there is synthesis of new RNA at different time points following RSC depletion. The results show that even after 1 hr of auxin, there is active transcription that is correlated with total mRNA levels at that time point (Figure S4C). Thus, the mRNA levels that we measure reflect recent (~5–10 min) transcriptional activity, supporting stronger involvement of RSC in transcription from mid-low-expressing genes.

Interestingly, we also found that the effect of RSC depletion on chromatin organization at promoters was more pronounced at lowly expressed genes (Figure 4C, top). Indeed, open NFRs of inactive and lowly expressed genes were filled faster and to a

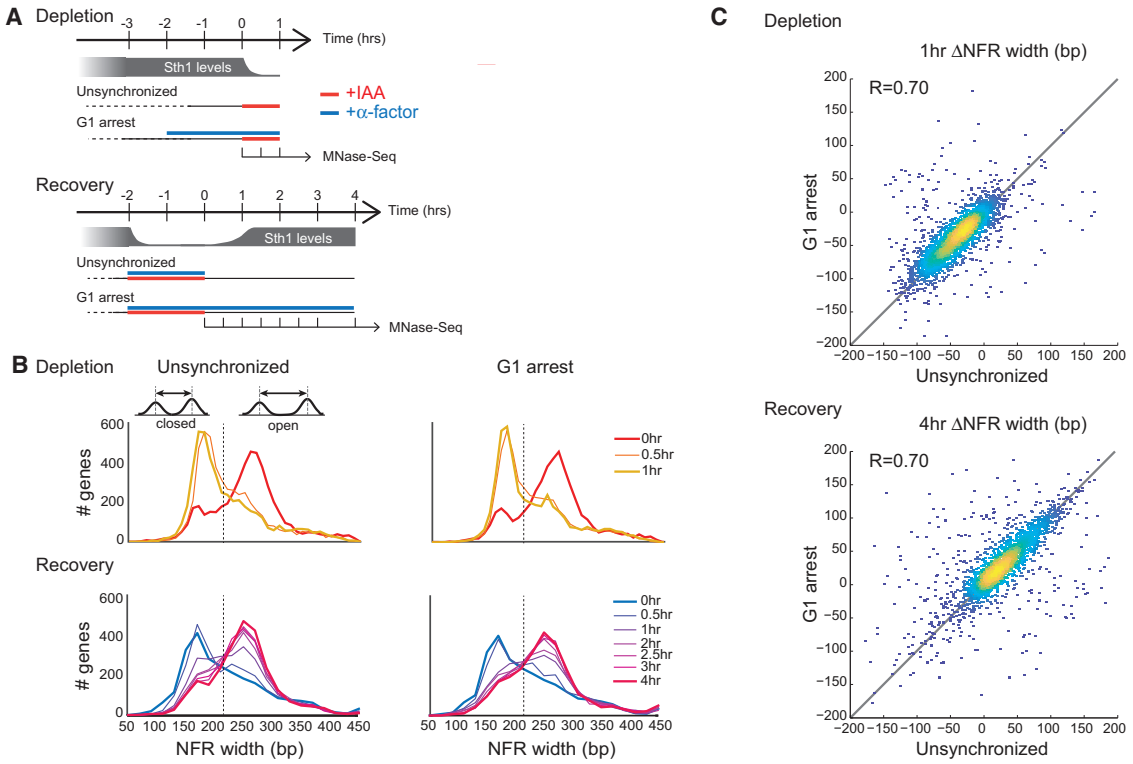

Figure 3. Sth1-Dependent NFR Clearing Is Replication Independent

(A) Experimental outline in G1-arrested cells. For depletion, yeast cells were grown to mid-log in YPD and incubated with or without alpha factor for 2 hr. At the indicated time, cells were transferred to a new tube, and Sth1 depletion was induced by auxin addition. All samples were fixed at the same time. For recovery, yeast cells were grown to mid-log in YPD and incubated with alpha-factor and auxin for 2 hr. Cells were washed and resuspended with or without alpha factor. MNase-seq was performed at the indicated time points.

(B) Distribution of NFR width in time course through Sth1 depletion (top) and recovery (bottom) in G1-arrested cells (right) and in unsynchronized cells (left).

(C) Density scatter of the change in NFR width for all genes through Sth1 depletion (1 hr, top) and recovery (4 hr, bottom), in G1 arrested versus unsynchronized cells.

See also Figure S3.

greater extent than those of highly expressed genes (Figure 4C, bottom). This difference is not due to GRF status of the NFR (Figure S4D). These observations suggest that RSC is active at inactive or weak promoters to maintain open NFRs and thus buffers the relationship between transcriptional activity and NFR promoter accessibility.

RSC Is Not Necessary for Stress-Responsive Induction

A chromatin remodeler can impact transcription in multiple ways. RSC maintains open NFRs, enabling access by the transcriptional machinery (Floer et al., 2010). In addition, RSC might have a direct role, being recruited by the transcriptional machinery upon induction to remodel promoter nucleosomes (Damelin et al., 2002; Lorch et al., 2011). Our experimental system allowed us to distinguish these two possibilities by examining cells that are depleted of Sth1 but have largely intact chromatin. To do this, we took advantage of a kinetic intermediate in our system, specifically after 20 min of auxin treatment, when Sth1 levels are already reduced but the chromatin is still mostly intact. We then measured the transcriptional response to stress (0.4 M KCl), measuring nucleosome occupancy and mRNA levels (Figure 4D). As a control, we examined a matching time course in cells with either one, but not both, of the auxin or stress treatments.

Contrary to our expectations (Damelin et al., 2002; Mas et al., 2009; Ng et al., 2002), cells depleted of Sth1 exhibited a virtually normal stress response. The strongly stress induced and repressed genes behaved similarly to cells with intact Sth1 at early time points (Figure 4E). However, as the cells acclimate to the osmotic stress, we see that the response of KCl+ IAA+ cells returned to profiles similar to IAA+ cells (Figure 4E).

To determine whether RSC-depleted cells exhibit normal stress-mediated chromatin alterations, we examined MNase profiles during the stress response (Figure 4F). We identified promoters of stress-induced genes whose nucleosome organization changed during stress response in normal cells. We classified these to three groups based on the type of changes: downstream shift of nucleosome +1, depletion of nucleosome +1, and depletion of nucleosome −1. Examining each group of promoters in Sth1-depleted cells we observe consistent changes in response to stress (Figure 4E).

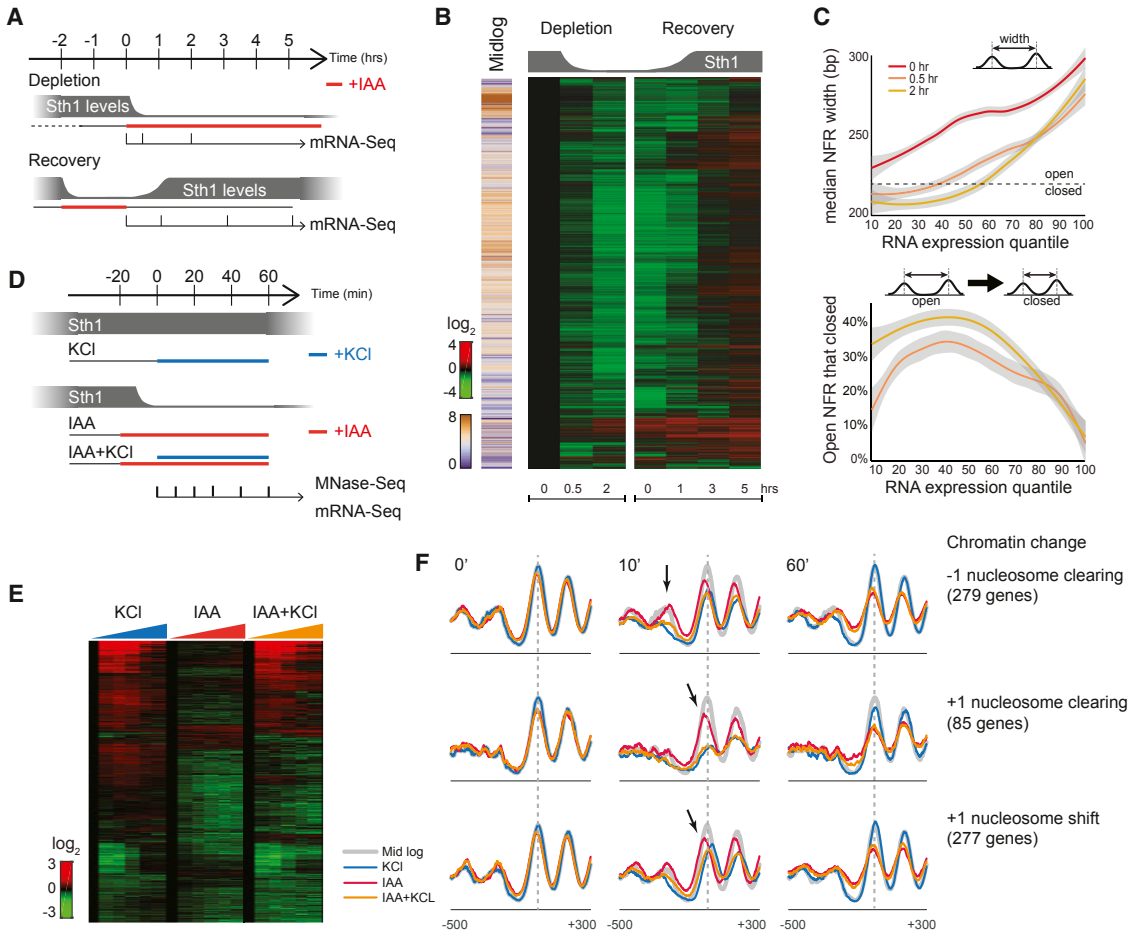

Figure 4. RSC Maintains Open NFRs in Lowly Expressed Genes but Is Not Necessary for an Acute Transcriptional Response

(A) Experiment outline (see Figure 2A).

(B) RNA fold change during Sth1 depletion and recovery. RNA level was normalized with *K. lactis* spike-in. Each row is a gene (5,529 genes), and each column is a sample. Heatmap is normalized to expression level prior to auxin addition (also mid-log). The levels of genes at this time are shown by the orange and purple columns.

(C) NFR width per RNA level. NFR width per RNA percentile in each sample (Loess smoothed) (top). Percentage of NFRs that closed in the presence of auxin for 0.5 hr (orange line) and 2 hr (yellow line) out of the NFRs that were open in steady state, per RNA percentile at the same time point (bottom).

(D) Stress experiment outline. Yeast cells were grown to mid-log in YPD. Auxin was added for 20 min, followed by salt addition (0.4 M KCl); samples were taken in time course and were subjected to MNase-seq and RNA sequencing (RNA-seq). Control samples without auxin or without KCL were performed.

(E) Heatmap of RNA fold change in three treatments: auxin only, salt only, and both salt and auxin. RNA levels are normalized per library. 2,322 clustered genes that change in response to the treatments are shown as fold change with respect to the matching expression at T = 0. Time points are indicated in the experiment outline (A).

(F) Metagene of subsets of stress-induced genes showing a typical response of chromatin structure to salt induction in time points in three treatments: auxin only, KCl only, and both KCl and auxin. Genes are positioned according to the nucleosome +1 center at T = 0. Black arrows mark location of changes.

See also Figure S4.

Together, these experiments show that Sth1-depleted cells exhibit largely normal stress responses in terms of gene induction and clearing of nucleosomes from their promoters. A straightforward interpretation is that Sth1 (RSC) is not a major factor for opening stress-responsive promoters. This suggests that other remodelers, such as Chd1 and SWI/SNF, might have a more prominent role for such induced remodeling (Shivaswamy and Iyer, 2008; Shivaswamy et al., 2008; Tsukiyama et al., 1999), while our data suggest that RSC's role is mostly in maintenance of potential promoters (as shown in Figure 4C). An alternative explanation we cannot currently exclude is that although Sth1 is depleted in these stress experiments, there are some residual levels in the cells. However, this would imply that because we observe almost normal promoter clearance, the few remaining molecules of Sth1 would have to be recruited highly efficiently to stress-responsive promoters.

Changes in the +1 Nucleosome Position Are Reflected in TSS Usage

The location of TSSs is tightly correlated with the position of the downstream +1 nucleosome. Several studies show that in yeast,

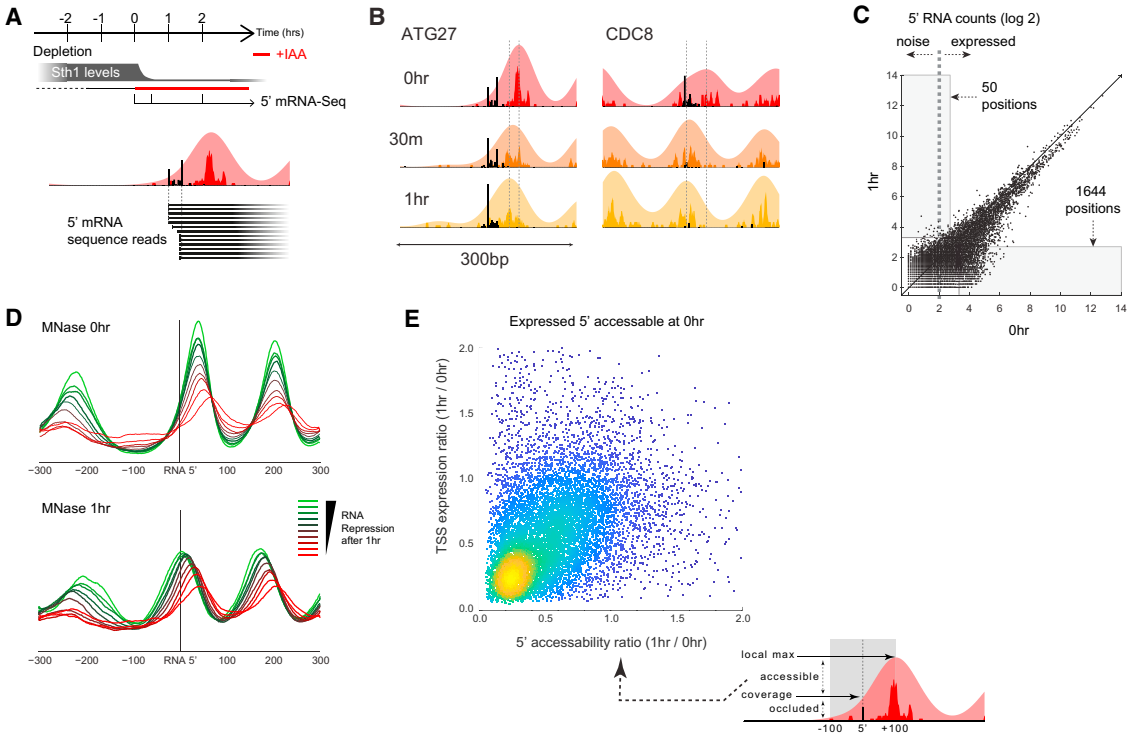

Figure 5. Changes in the +1 Nucleosome Position Are Reflected in TSS Usage

(A) Experimental outline (as in Figure 2A). An example of the data representation showing RNA 5′ ends (black), MNase read centers (dark red), and coverage (light red) around the TSS.

(B) Nucleosome positioning and 5′ RNA ends during Sth1 depletion in CDC8 and ATG27 promoters. Dashed lines represent peak centers before and 1 hr after auxin addition.

(C) 5′ RNA level at each position over the genome before and after Sth1 depletion (normalized with *K. lactis* spike-in).

(D) Median nucleosome positioning around mRNA 5′ ends before (top) and 1 hr after (bottom) auxin addition. mRNA 5′ positions are separated to groups according to their fold change following Sth1 depletion.

(E) Change in expression (1 hr/0 hr) versus change in accessibility (1 hr/0 hr) for mRNA 5′ locations that are expressed (Figure 5C) and accessible (Figure S5B) before auxin addition.

See also Figure S5.

TSSs are located 10–15 bp into the nucleosome or ~60 bp from the nucleosome dyad (reviewed in Jiang and Pugh, 2009b). It was suggested that the +1 nucleosome determines the location of the TSS, at least for TATA-less promoters, potentially by impeding RNA polymerase II (Pol II) scanning (Rhee and Pugh 2012). Thus, movement of the +1 nucleosome toward the NFR in RSC-depleted cells is expected to impact the TSS.

To examine this directly, we performed 5′ RNA-seq (STAR Methods) during RSC-depletion (Figure 5A; STAR Methods). Consistent with previous reports (Miura et al., 2006; Pelechano et al., 2013; Rojas-Duran and Gilbert, 2012), we observed multiple 5′ start sites at most genes (for example Figure 5B, top row). For some genes, there is a single dominant TSS (e.g., CDC8), and for other genes, there are multiple major TSSs (e.g., ATG27). Most TSS are positioned ~45 bp upstream of nucleosome centers (Figure S5A), consistent with prior observations (Jiang and Pugh, 2009b). In particular, for most genes, the location of the PIC is at a fixed distance from the +1 nucleosome (Rhee and Pugh, 2012). However, there is a class of TSS positions (20%) that violate this rule and overlap with nucleosome centers (Figures S5A and S5B). There are several possible explanations for this inconsistency. First, the observed nucleosome-center-overlapping TSSs could indicate locations where there is heterogeneity in the population. Indeed, in genes with a high fraction of occluded TSSs, nucleosome +1 tends to be fuzzier (Figure S5C). Second, these locations are enriched (38%, $p < 10^{-18}$) in TATA-binding protein associated factor (TAF)-depleted genes (Rhee and Pugh, 2012), where the PIC to +1 nucleosome distance is not conserved. Additionally, ~33% ($p < 10^{-11}$) of the genes associated with these locations are noisy genes where transcription is bursty (Bar-Even et al., 2006; Newman et al., 2006).

Upon RSC depletion, we observe changes in TSS patterns at promoters (Figure 5B). For example, in ATG27, where there are two dominant TSSs, the downstream TSS is repressed after RSC depletion, while the upstream one is maintained. In contrast, in CDC8 the single dominant TSS is repressed during the depletion, and the gene becomes totally repressed. In both cases, the repression is consistent with the upstream shift of the +1 nucleosome (Figure 5B).

We wondered whether the repressed TSSs are always accompanied by corresponding nucleosome shifts as in the examples of Figure 5B. We compared 5′ RNA-seq before and 1 hr after introduction of auxin. We used *K. lactis* spike-in to normalize the two samples (STAR Methods). Consistent with our earlier 3′ RNA-seq, we observed a global reduction in TSS usage after RSC depletion (Figure 5C). We now asked whether repressed TSSs are accompanied by different nucleosome movement than ones that are maintained. To test that, we created a profile of nucleosome center occupancy aligned to the TSS sites. Partitioning TSSs by their response to RSC depletion (Figure 5D), the degree of repression is correlated with the degree of shift in the downstream (+1) nucleosome position. Highly repressed TSSs are occluded by nucleosomes, while unrepressed TSSs show only minor changes in the +1 nucleosome position. Comparing change in TSS expression to change in nucleosome overlap (Figure 5E), we see a general agreement. Moreover, there are two noticeable subpopulations, one that is highly repressed while being occluded and another that is not occluded and only mildly repressed. Examining where these TSSs are located with respect to alternate TSSs for the same genes, we see that the repressed subpopulation is enriched with downstream TSS positions, while the unrepressed genes is enriched by upstream TSS positions (Figure S5D).

Previous literature suggested a "ruler" model, in which TSS position was determined by nucleosome location (Hughes et al., 2012; Li et al., 1994; Rhee and Pugh, 2012). Such a model predicts that shifts in nucleosome positions would be accompanied by introduction of new TSSs. Comparing the level of expression from each 5′ site in the genome before and after RSC depletion (Figure 5C), we observe a large number of repressed sites (~2,500 sites) and a scarce number of new sites (~100 sites). Thus, RSC depletion and subsequent nucleosome relocation did not expose new TSSs, even in cases where the nucleosome shift seem to be homogeneous in the population. This is consistent with the observation of NFR fill-in from both ends. Thus, a shift in the −1 nucleosome toward the NFR usually occludes potential upstream TSSs.

Changes in 5′ TSS Accessibility Are Indicative of Changes in Gene Expression Levels

Our results demonstrate a wide range of changes in the activity of individual TSSs upon Sth1 depletion. Since many genes have multiple alternative TSSs (Miura et al., 2006; Pelechano et al., 2013), we wondered how these changes are reflected in the overall expression of transcripts. We observed that there is mostly TSS loss upon RSC depletion. Thus, each gene is associated with a set of TSS positions, and following RSC depletion, a subset of these TSS positions are repressed. A naive model is one where gene expression following RSC depletion is determined by removal of the contribution of repressed TSSs (Figure 6A). Indeed, genes that retain expression following depletion tend to have alternative TSSs that are not obscured by nucleosome movement (Figure S6). These TSS positions are still transcribed even though nucleosome +1 moved toward the NFR. This model also does not address genes whose TSSs overlap with nucleosome-occupied regions already at time 0 (see above).

To test the relevance of this simple model, we estimated for each TSS the degree it is obscured by nucleosomes following RSC depletion and calculated for each gene the amount of TSS activity it retains after RSC depletion as the sum across all associated TSS positions (Figure 6A). For example, all CDC8 TSSs active at time 0 are repressed after 1 hr in auxin. In contrast, ATG27 partially loses 4 out of 10 TSS positions, retaining 44% of possible expression. Surprisingly, this naive model explains 72% of the variation after 1 hr of RSC depletion (Figure 6B).

One issue that our data do not resolve is whether RSC is necessary for TBP binding and PIC assembly at each of the promoters (Kubik et al., 2018). The promoters of these genes where there are still productive TSSs are presumably bound by TBP and PIC to enable transcription from these remaining TSSs. On the other hand, in genes that do not retain expression following RSC depletion and nucleosome movement, our data cannot determine whether the PIC is able to bind (and is blocked from initiation) or fails to bind following RSC depletion.

DISCUSSION

Here, we studied the role of ATP-dependent chromatin remodelers in nucleosome positioning. Addressing this question *in vivo* is complicated for several reasons. Some of the ATPase units of chromatin remodelers are essential. Moreover, as with all chromatin-related factors, remodeler action is potentially pervasive throughout the genome and can have dramatic global indirect effects. Consequently, chromatin remodelers are involved in many cellular processes, and therefore it is difficult to distinguish their direct and indirect effects. Our strategy to circumvent these complications is to use a conditional depletion system that rapidly (~20 min) clears most of the target protein.

We screened all ATP-dependent chromatin remodelers in budding yeast, and we found the most dramatic changes in nucleosome positions are upon depletion of Sth1, the catalytic subunit of the RSC complex. We therefore examined in detail the dynamics of changes upon Sth1 depletion and recovery. We examined the role of DNA replication and transcription in these processes, assaying both nucleosome positions and mRNA levels during RSC depletion and recovery. We find close but non-trivial interplay between transcription and RSC-dependent nucleosome positioning.

Limitations of Conditional Depletion

Our results were obtained using the AID system, in which an AID tag is added at the end of a target gene to form an AID-tagged protein. The rapid induced degradation is much faster than transcriptional repression and does not involve cellular perturbations as in temperature sensitive (TS) alleles (Hartley and Madhani, 2009; Parnell et al., 2008, 2015). Moreover, in contrast to the rapid anchor-away system (Kubik et al., 2018), this system also allows to study recovery of the protein.

However, this system has some caveats. The depletion is not absolute as new copies of the target protein are continuously synthesized and degraded. Incomplete degradation can introduce heterogeneity among cells. In preliminary experiments using an AID-GFP tag, we examined GFP loss with live-cell

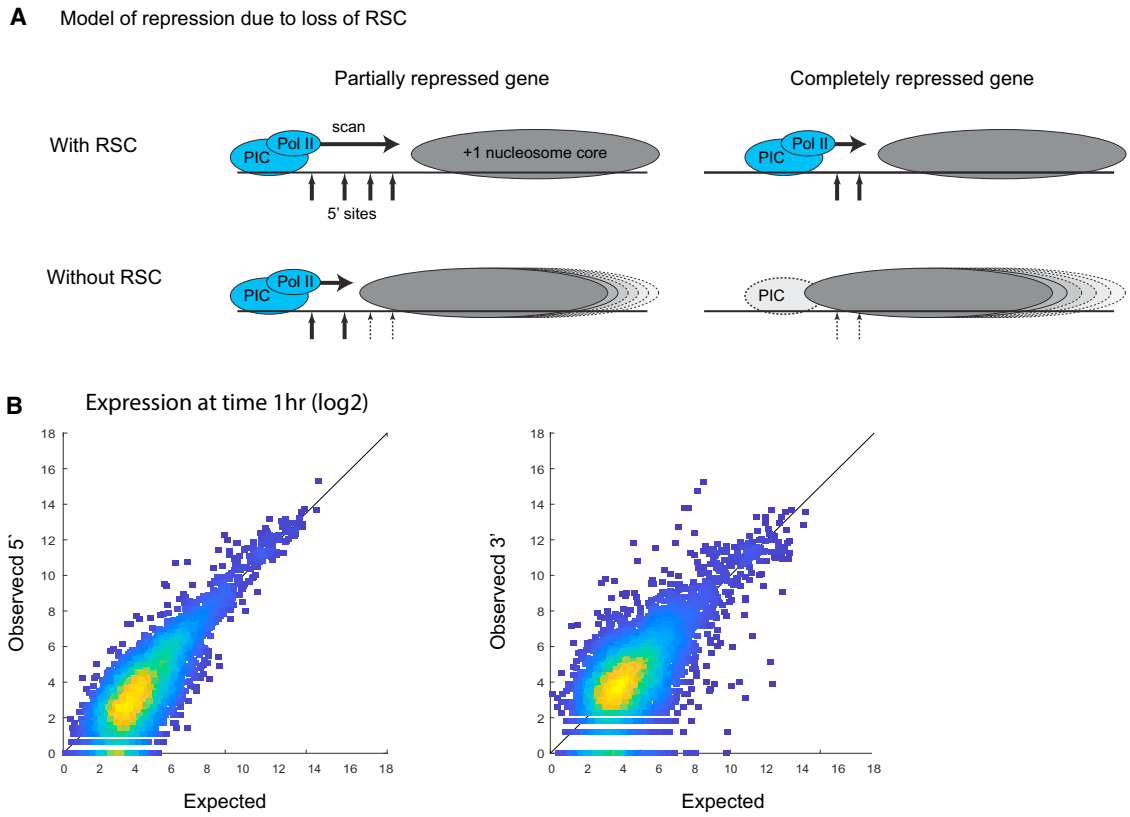

Figure 6. Changes in 5′ TSS Accessibility Are Indicative of Changes in Gene Expression Levels

(A) A model. In the presence of RSC, transcription starts at specific positions in a range upstream of the +1 nucleosome. When Sth1 is removed, some TSSs are maintained and others are inaccessible, resulting in different repression levels.

(B) Scatter of observed versus expected RNA level per gene (3,920 genes are shown) 1 hr after Sth1 depletion. Observed level is from 5′ RNA (left) or 3′ RNA (right) sequencing data. Expected level is calculated by 5′ RNA level before Sth1 depletion and change in the accessibility of its TSS positions (STAR Methods). See also Figure S6.

time-lapse microscopy and observed rapid loss of fluorescence following introduction of auxin in all cells (data not shown). We also observed a complete, synchronous shift in nucleosome positions at many loci (e.g., Figure 2C), inconsistent with the presence of heterogeneous populations.

Another concern could be that the addition of C-terminal tags could disrupt protein function. Comparing nucleosome positioning in a wild-type (WT) strain to our AID-tagged strains in the absence of auxin, we see a small effect on nucleosome positioning (Figure S1). Combined with the dramatic effects following introduction of auxin, these data suggest that the tagged Sth1 maintains most of its functionality.

Timescales of Depletion and Recovery

The rapid degradation system allowed us to monitor nucleosome dynamics through RSC depletion at a fine temporal resolution. Previous work has shown increased overlap of nucleosomes with NFRs following RSC depletion (Hartley and Madhani, 2009; Kubik et al., 2018; Parnell et al., 2008). These works mostly focused on either a few loci or genome-wide at a single time point following the depletion. We show that the gain of nucleosomes starts already 10–20 min after the addition of auxin and in most genes converges within 45 min. The NFR fill-in was dramatic and occurred in most genes in these genome-scale experiments. This dramatic change in this short timescale is surprising and suggests that RSC is already below its critical level by 10 min after the induction. It also suggests that RSC is constantly active within the cell at most promoters.

The process of recovery of chromatin structure was slower than depletion. The convergence of recovery was seen 2 hr after auxin was washed from the media. The recovery process involves intracellular auxin depletion, Sth1 synthesis, folding, and complex assembly, all of which presumably take longer than degradation. These processes may account for the initial delay we observe before restoration of the chromatin state begins.

Replication and Nucleosome Positioning

The global nature of the changes in chromatin structure in response to Sth1 depletion raised the possibility of involvement of the DNA replication machinery. Indeed, it was previously shown that Sth1-dependent chromatin changes at one Pol-III gene (*SCR1*) are replication-dependent (Parnell et al., 2008). DNA replication involves major disruptions via chromatin

disassembly and reestablishment of the nucleosome template following replication fork passage (Kaufman and Rando, 2010). Therefore, we tested whether the effects of RSC depletion depended on passage through S phase. We provide strong evidence that this is not the case. Specifically, we found that depletion and recovery of Sth1 had the same effects in asynchronous or in G1-arrested cells, indicating that RSC's activity in clearing nucleosomes from NFRs is replication independent. These results are consistent with *in vitro* observations that RSC remodels nucleosomes without replication-dependent disassembly (Krietenstein et al., 2016).

Chromatin Memory

We used our degron system to wash auxin from the media and investigate chromatin dynamics following Sth1 re-accumulation. As was previously shown with TS allele Sth1, the effect of Sth1 depletion on cell growth is reversible (Parnell et al., 2008). The induced degron system allowed us to follow Sth1 re-accumulation without additional perturbations to the cells. Although total cell state (chromatin, transcription, and additional processes) after depletion was radically different, chromatin structure and the transcriptional state completely recovered upon RSC re-accumulation. To our surprise, full recovery of chromatin was independent of replication. The complete recovery of chromatin structure raises significant questions: What are the factors and features that hold the information that enable nucleosome repositioning? Which additional change in cell state will prevent the recovery of nucleosome positioning? Presumably, each promoter holds a combination of transcription factors, chromatin remodeling complexes, and sequence features that direct the recovery of nucleosome positioning by RSC. Identifying the most significant "bookmarks" *in vivo* remains an open challenge.

NFR Width and Transcription

Combining nucleosome positioning assays and RNA-seq, we examined the correlation between transcription and chromatin structure around the NFR upon RSC depletion. In addition to NFR fill-in, depletion of Sth1 leads to global reductions in RNA levels. Both transcription level and NFR structure recovered following Sth1 re-accumulation to a native state. The correlation between NFR width and gene expression levels has been reported (Rando and Winston, 2012; Weiner et al., 2010). However, this correlation is not perfect, and many low-expressed genes maintain an open NFR. Interestingly, the effect of RSC depletion on NFR width in these genes was even more pronounced (Ganguli et al., 2014). We thus conclude that lowly expressed genes maintain an open NFR in an RSC-dependent manner. Maintaining an open NFR could be an advantage in regulating low-expressed constitutive genes (Tirosh and Barkai, 2008).

In contrast, the NFR width of highly transcribed genes is less affected by RSC depletion. This could be due to the activity of Pol II and other transcription-related proteins at these NFRs. Alternatively, these promoters are better at recruitment of RSC and manage to recruit residual functioning RSC, while other genes do not. This scenario is somewhat incompatible with the timescales of the changes. Moreover, if imperfect recruitment would most probably incur population heterogeneity, leading to fuzzy nucleosome positioning at these NFRs, which we do not observe in these promoters.

Since we have shown that RSC is capable to drive the formation of and maintain an open NFR, we hypothesized it has a role in transcription activation in response to stress. Indeed, it was previously shown that RSC is required for stress-induced activation of a small subset of genes (Damelin et al., 2002; Mas et al., 2009). To distinguish between direct and indirect effects of RSC depletion, stress was induced only 20 min after auxin was added, when RSC is already depleted from cells but its effect is still minor. Interestingly, RSC depletion did not affect transcription activation and had minimal effect on NFR clearance in response to stress, suggesting that RSC is not required for gene activation following stress. (Figure 4F). We cannot exclude that residual RSC is recruited to the stress promoters following stress induction. However, since promoter clearance following stress induction is almost normal in the absence of RSC, it is more probable that stress induction is independent of RSC.

We conclude that RSC has a role in the formation of a proper chromatin state to enable the activation of transcription, especially in low-expressed genes. It is not necessary for the clearance of promoters and activation of gene expression in response to stress. Other remodelers, such as Chd1 and SWI/SNF, might be responsible for such induced remodeling, possibly in redundancy with RSC.

Transcription Initiation and the +1 Nucleosome Position

RSC depletion affects both transcription and NFR width. However, the causality linking these is unclear. Does NFR fill-in prevent transcription, or is transcription required for NFR maintenance. Previous work argued against NFR fill-in due to loss of transcription, since transcriptional arrest causes movement of +1 nucleosomes downstream into the gene body, opposite to the nucleosome movement observed in RSC-depleted cells (Kubik et al., 2018; Parnell et al., 2008; Weiner et al., 2010). The location of TSSs in yeast is tightly correlated with the position of the downstream +1 nucleosome. Therefore, we hypothesized that the decrease in RNA level was a result of the gain of nucleosomes in the NFR. Indeed, we find that changes in nucleosome positions are tightly correlated to the specific TSS usage at promoters. Upon RSC depletion, we observe inactivation of TSSs that are covered by nucleosomes, supporting the hypothesis that nucleosomes prevent transcription *in vivo* (Hartley and Madhani, 2009; Parnell et al., 2008; Spain et al., 2014). Moreover, upstream TSSs that are not covered by nucleosomes continue to transcribe, suggesting that the transcription machinery is still functional. To our surprise, we did not find newly formed TSSs following the repositioning of the +1 nucleosome. Other limiting factors, GRFs, or movement of the −1 nucleosome might prevent new potential TSSs from transcribing.

We conclude that the depletion of RSC allows nucleosomes to accumulate in NFRs, leading to TSS occlusion and inactivation and eventually to a decrease in gene expression. More generally, we can consider two modes of occlusion (Figure 6A). In the first, occlusion by the nucleosome blocks PIC formation. In the second, the PIC is formed but nucleosome occlusion blocks the TSS scan. Clearly, for some genes, such as CDC8, RSC depletion leads to closing of the NFR, which is consistent with lower levels

of TBP and PIC formation (Kubik et al., 2018). For others, such as ATG27, we conclude that PIC formation is not hampered by nucleosomes. We cannot rule out cases where there are multiple PIC positions in the NFR. However, ChIP-exo of PIC components suggests a single dominant PIC location (Rhee and Pugh, 2012).

STAR★METHODS

Detailed methods are provided in the online version of this paper and include the following:

- KEY RESOURCES TABLE
- CONTACT FOR REAGENT AND RESOURCE SHARING
- EXPERIMENTAL MODEL AND SUBJECT DETAILS
- METHOD DETAILS
  - MNase digestion and DNA Sequencing
  - RNA purification and 3′-Library preparation
  - Metabolic labeling and SLAM-Seq
  - 5′-Library preparation
- QUANTIFICATION AND STATISTICAL ANALYSIS
  - Nucleosome mapping and features
  - 3′ RNA data - Sequence Analysis
  - 5′ RNA data analysis
- DATA AND SOFTWARE AVAILABILITY

SUPPLEMENTAL INFORMATION

Supplemental Information includes six figures and can be found with this article online at https://doi.org/10.1016/j.celrep.2018.12.020.

ACKNOWLEDGMENTS

We thank I. Amit for reagents and his help in establishing MNase-seq and RNA-seq systems. We thank H. Ulrich for plasmids and yeast strains. We thank P. Kaufman, D. Engelberg, O. Rando, T. Kaplan, I. Amit, and current and past members of the Friedman lab for comments and discussion. This work was funded by grants from the European Research Council (ERC AdG grant 340712, "ChromatinSys") and by The Israel Science Foundation (I-CORE on "Chromatin and RNA in gene regulation").

AUTHOR CONTRIBUTIONS

Conceptualization, A.K.-B., D.J.-S., and N.F.; Methodology and Investigation, D.J.-S., and A.K.-B.; Software and Formal Analysis, A.K.-B.; Resources, A.A. and D.J.-S. (SLAM-seq data); Writing and Visualization, N.F., A.K.-B., D.J.-S., and A.A.; Supervision and Funding Acquisition, N.F.

DECLARATION OF INTERESTS

The authors declare no competing interests.

Received: August 16, 2018
Revised: November 19, 2018
Accepted: December 4, 2018
Published: January 2, 2019

REFERENCES

Bar-Even, A., Paulsson, J., Maheshri, N., Carmi, M., O'Shea, E., Pilpel, Y., and Barkai, N. (2006). Noise in protein expression scales with natural protein abundance. Nat. Genet. *38*, 636–643.

Bell, O., Tiwari, V.K., Thomä, N.H., and Schübeler, D. (2011). Determinants and dynamics of genome accessibility. Nat. Rev. Genet. *12*, 554–564.

Blecher-Gonen, R., Barnett-Itzhaki, Z., Jaitin, D., Amann-Zalcenstein, D., Lara-Astiaso, D., and Amit, I. (2013). High-throughput chromatin immunoprecipitation for genome-wide mapping of in vivo protein-DNA interactions and epigenomic states. Nat. Protoc. *8*, 539–554.

Bucceri, A., Kapitza, K., and Thoma, F. (2006). Rapid accessibility of nucleosomal DNA in yeast on a second time scale. EMBO J. *25*, 3123–3132.

Cairns, B.R., Lorch, Y., Li, Y., Zhang, M., Lacomis, L., Erdjument-Bromage, H., Tempst, P., Du, J., Laurent, B., and Kornberg, R.D. (1996). RSC, an essential, abundant chromatin-remodeling complex. Cell *87*, 1249–1260.

Chaban, Y., Ezeokonkwo, C., Chung, W.-H., Zhang, F., Kornberg, R.D., Maier-Davis, B., Lorch, Y., and Asturias, F.J. (2008). Structure of a RSC-nucleosome complex and insights into chromatin remodeling. Nat. Struct. Mol. Biol. *15*, 1272–1277.

Chai, B., Huang, J., Cairns, B.R., and Laurent, B.C. (2005). Distinct roles for the RSC and Swi/Snf ATP-dependent chromatin remodelers in DNA double-strand break repair. Genes Dev. *19*, 1656–1661.

Clapier, C.R., and Cairns, B.R. (2009). The biology of chromatin remodeling complexes. Annu. Rev. Biochem. *78*, 273–304.

Damelin, M., Simon, I., Moy, T.I., Wilson, B., Komili, S., Tempst, P., Roth, F.P., Young, R.A., Cairns, B.R., and Silver, P.A. (2002). The genome-wide localization of Rsc9, a component of the RSC chromatin-remodeling complex, changes in response to stress. Mol. Cell *9*, 563–573.

Du, J., Nasir, I., Benton, B.K., Kladde, M.P., and Laurent, B.C. (1998). Sth1p, a Saccharomyces cerevisiae Snf2p/Swi2p homolog, is an essential ATPase in RSC and differs from Snf/Swi in its interactions with histones and chromatin-associated proteins. Genetics *150*, 987–1005.

Dye, B.T., Hao, L., and Ahlquist, P. (2005). High-throughput isolation of Saccharomyces cerevisiae RNA. Biotechniques *38*, 868–870.

Field, Y., Kaplan, N., Fondufe-Mittendorf, Y., Moore, I.K., Sharon, E., Lubling, Y., Widom, J., and Segal, E. (2008). Distinct modes of regulation by chromatin encoded through nucleosome positioning signals. PLoS Comput. Biol. *4*, e1000216.

Floer, M., Wang, X., Prabhu, V., Berrozpe, G., Narayan, S., Spagna, D., Alvarez, D., Kendall, J., Krasnitz, A., Stepansky, A., et al. (2010). A RSC/nucleosome complex determines chromatin architecture and facilitates activator binding. Cell *141*, 407–418.

Ganguli, D., Chereji, R.V., Iben, J.R., Cole, H.A., and Clark, D.J. (2014). RSC-dependent constructive and destructive interference between opposing arrays of phased nucleosomes in yeast. Genome Res. *24*, 1637–1649.

Gkikopoulos, T., Schofield, P., Singh, V., Pinskaya, M., Mellor, J., Smolle, M., Workman, J.L., Barton, G.J., and Owen-Hughes, T. (2011). A role for Snf2-related nucleosome-spacing enzymes in genome-wide nucleosome organization. Science *333*, 1758–1760.

Gutin, J., Sadeh, R., Bodenheimer, N., Joseph-Strauss, D., Klein-Brill, A., Alajem, A., Ram, O., and Friedman, N. (2018). Fine-resolution mapping of TF binding and chromatin interactions. Cell Rep. *22*, 2797–2807.

Han, M., and Grunstein, M. (1988). Nucleosome loss activates yeast downstream promoters in vivo. Cell *55*, 1137–1145.

Hartley, P.D., and Madhani, H.D. (2009). Mechanisms that specify promoter nucleosome location and identity. Cell *137*, 445–458.

Herzog, V.A., Reichholf, B., Neumann, T., Rescheneder, P., Bhat, P., Burkard, T.R., Wlotzka, W., von Haeseler, A., Zuber, J., and Ameres, S.L. (2017). Thiol-linked alkylation of RNA to assess expression dynamics. Nat. Methods *14*, 1198–1204.

Hsu, J.-M., Huang, J., Meluh, P.B., and Laurent, B.C. (2003). The yeast RSC chromatin-remodeling complex is required for kinetochore function in chromosome segregation. Mol. Cell. Biol. *23*, 3202–3215.

Hughes, A.L., Jin, Y., Rando, O.J., and Struhl, K. (2012). A functional evolutionary approach to identify determinants of nucleosome positioning: a unifying model for establishing the genome-wide pattern. Mol. Cell *48*, 5–15.

Jiang, C., and Pugh, B.F. (2009a). A compiled and systematic reference map of nucleosome positions across the Saccharomyces cerevisiae genome. Genome Biol. *10*, R109.

Jiang, C., and Pugh, B.F. (2009b). Nucleosome positioning and gene regulation: advances through genomics. Nat. Rev. Genet. *10*, 161–172.

Kaufman, P.D., and Rando, O.J. (2010). Chromatin as a potential carrier of heritable information. Curr. Opin. Cell Biol. *22*, 284–290.

Kornberg, R.D. (1974). Chromatin structure: a repeating unit of histones and DNA. Science *184*, 868–871.

Krietenstein, N., Wal, M., Watanabe, S., Park, B., Peterson, C.L., Pugh, B.F., and Korber, P. (2016). Genomic Nucleosome Organization Reconstituted with Pure Proteins. Cell *167*, 709–721.e12.

Kubik, S., O'Duibhir, E., de Jonge, W.J., Mattarocci, S., Albert, B., Falcone, J.-L., Bruzzone, M.J., Holstege, F.C.P., and Shore, D. (2018). Sequence-directed action of RSC remodeler and general regulatory factors modulates+1 nucleosome position to facilitate transcription. Mol. Cell *71*, 89–102.e5.

Langmead, B., and Salzberg, S.L. (2012). Fast gapped-read alignment with Bowtie 2. Nat. Methods *9*, 357–359.

Lee, W., Tillo, D., Bray, N., Morse, R.H., Davis, R.W., Hughes, T.R., and Nislow, C. (2007). A high-resolution atlas of nucleosome occupancy in yeast. Nat. Genet. *39*, 1235–1244.

Li, Y., Flanagan, P.M., Tschochner, H., and Kornberg, R.D. (1994). RNA polymerase II initiation factor interactions and transcription start site selection. Science *263*, 805–807.

Li, H., Handsaker, B., Wysoker, A., Fennell, T., Ruan, J., Homer, N., Marth, G., Abecasis, G., and Durbin, R.; 1000 Genome Project Data Processing Subgroup (2009). The Sequence Alignment/Map format and SAMtools. Bioinformatics *25*, 2078–2079.

Lohr, D. (1997). Nucleosome transactions on the promoters of the yeast GAL and PHO genes. J. Biol. Chem. *272*, 26795–26798.

Lorch, Y., LaPointe, J.W., and Kornberg, R.D. (1987). Nucleosomes inhibit the initiation of transcription but allow chain elongation with the displacement of histones. Cell *49*, 203–210.

Lorch, Y., Zhang, M., and Kornberg, R.D. (1999). Histone octamer transfer by a chromatin-remodeling complex. Cell *96*, 389–392.

Lorch, Y., Griesenbeck, J., Boeger, H., Maier-Davis, B., and Kornberg, R.D. (2011). Selective removal of promoter nucleosomes by the RSC chromatin-remodeling complex. Nat. Struct. Mol. Biol. *18*, 881–885.

Lorch, Y., Maier-Davis, B., and Kornberg, R.D. (2014). Role of DNA sequence in chromatin remodeling and the formation of nucleosome-free regions. Genes Dev. *28*, 2492–2497.

Mas, G., de Nadal, E., Dechant, R., Rodríguez de la Concepción, M.L., Logie, C., Jimeno-González, S., Chávez, S., Ammerer, G., and Posas, F. (2009). Recruitment of a chromatin remodelling complex by the Hog1 MAP kinase to stress genes. EMBO J. *28*, 326–336.

Méchali, M. (2010). Eukaryotic DNA replication origins: many choices for appropriate answers. Nat. Rev. Mol. Cell Biol. *11*, 728–738.

Miura, F., Kawaguchi, N., Sese, J., Toyoda, A., Hattori, M., Morishita, S., and Ito, T. (2006). A large-scale full-length cDNA analysis to explore the budding yeast transcriptome. Proc. Natl. Acad. Sci. USA *103*, 17846–17851.

Montel, F., Castelnovo, M., Menoni, H., Angelov, D., Dimitrov, S., and Faivre-Moskalenko, C. (2011). RSC remodeling of oligo-nucleosomes: an atomic force microscopy study. Nucleic Acids Res. *39*, 2571–2579.

Morawska, M., and Ulrich, H.D. (2013). An expanded tool kit for the auxin-inducible degron system in budding yeast. Yeast *30*, 341–351.

Newman, J.R.S., Ghaemmaghami, S., Ihmels, J., Breslow, D.K., Noble, M., DeRisi, J.L., and Weissman, J.S. (2006). Single-cell proteomic analysis of S. cerevisiae reveals the architecture of biological noise. Nature *441*, 840–846.

Ng, H.H., Robert, F., Young, R.A., and Struhl, K. (2002). Genome-wide location and regulated recruitment of the RSC nucleosome-remodeling complex. Genes Dev. *16*, 806–819.

Nishimura, K., Fukagawa, T., Takisawa, H., Kakimoto, T., and Kanemaki, M. (2009). An auxin-based degron system for the rapid depletion of proteins in nonplant cells. Nat. Methods *6*, 917–922.

Ocampo, J., Chereji, R.V., Eriksson, P.R., and Clark, D.J. (2016). The ISW1 and CHD1 ATP-dependent chromatin remodelers compete to set nucleosome spacing in vivo. Nucleic Acids Res. *44*, 4625–4635.

Ozonov, E.A., and van Nimwegen, E. (2013). Nucleosome free regions in yeast promoters result from competitive binding of transcription factors that interact with chromatin modifiers. PLoS Comput. Biol. *9*, e1003181.

Parnell, T.J., Huff, J.T., and Cairns, B.R. (2008). RSC regulates nucleosome positioning at Pol II genes and density at Pol III genes. EMBO J. *27*, 100–110.

Parnell, T.J., Schlichter, A., Wilson, B.G., and Cairns, B.R. (2015). The chromatin remodelers RSC and ISW1 display functional and chromatin-based promoter antagonism. eLife *4*, e06073.

Pelechano, V., Wei, W., and Steinmetz, L.M. (2013). Extensive transcriptional heterogeneity revealed by isoform profiling. Nature *497*, 127–131.

Picelli, S., Björklund, A.K., Reinius, B., Sagasser, S., Winberg, G., and Sandberg, R. (2014a). Tn5 transposase and tagmentation procedures for massively scaled sequencing projects. Genome Res. *24*, 2033–2040.

Picelli, S., Faridani, O.R., Björklund, A.K., Winberg, G., Sagasser, S., and Sandberg, R. (2014b). Full-length RNA-seq from single cells using Smart-seq2. Nat. Protoc. *9*, 171–181.

Ramachandran, S., Zentner, G.E., and Henikoff, S. (2015). Asymmetric nucleosomes flank promoters in the budding yeast genome. Genome Res. *25*, 381–390.

Rando, O.J., and Winston, F. (2012). Chromatin and transcription in yeast. Genetics *190*, 351–387.

Rhee, H.S., and Pugh, B.F. (2012). Genome-wide structure and organization of eukaryotic pre-initiation complexes. Nature *483*, 295–301.

Rojas-Duran, M.F., and Gilbert, W.V. (2012). Alternative transcription start site selection leads to large differences in translation activity in yeast. RNA *18*, 2299–2305.

Shivaswamy, S., and Iyer, V.R. (2008). Stress-dependent dynamics of global chromatin remodeling in yeast: dual role for SWI/SNF in the heat shock stress response. Mol. Cell. Biol. *28*, 2221–2234.

Shivaswamy, S., Bhinge, A., Zhao, Y., Jones, S., Hirst, M., and Iyer, V.R. (2008). Dynamic remodeling of individual nucleosomes across a eukaryotic genome in response to transcriptional perturbation. PLoS Biol. *6*, e65.

Simic, R., Lindstrom, D.L., Tran, H.G., Roinick, K.L., Costa, P.J., Johnson, A.D., Hartzog, G.A., and Arndt, K.M. (2003). Chromatin remodeling protein Chd1 interacts with transcription elongation factors and localizes to transcribed genes. EMBO J. *22*, 1846–1856.

Spain, M.M., Ansari, S.A., Pathak, R., Palumbo, M.J., Morse, R.H., and Govind, C.K. (2014). The RSC complex localizes to coding sequences to regulate Pol II and histone occupancy. Mol. Cell *56*, 653–666.

Tirosh, I., and Barkai, N. (2008). Two strategies for gene regulation by promoter nucleosomes. Genome Res. *18*, 1084–1091.

Tirosh, I., Sigal, N., and Barkai, N. (2010). Widespread remodeling of mid-coding sequence nucleosomes by Isw1. Genome Biol. *11*, R49.

Tsukiyama, T., Palmer, J., Landel, C.C., Shiloach, J., and Wu, C. (1999). Characterization of the imitation switch subfamily of ATP-dependent chromatin-remodeling factors in Saccharomyces cerevisiae. Genes Dev. *13*, 686–697.

Voichek, Y., Bar-Ziv, R., and Barkai, N. (2016). Expression homeostasis during DNA replication. Science *351*, 1087–1090.

Weiner, A., Hughes, A., Yassour, M., Rando, O.J., and Friedman, N. (2010). High-resolution nucleosome mapping reveals transcription-dependent promoter packaging. Genome Res. *20*, 90–100.

Weiner, A., Hsieh, T.-H.S., Appleboim, A., Chen, H.V., Rahat, A., Amit, I., Rando, O.J., and Friedman, N. (2015). High-resolution chromatin dynamics during a yeast stress response. Mol. Cell *58*, 371–386.

Whitehouse, I., Rando, O.J., Delrow, J., and Tsukiyama, T. (2007). Chromatin remodelling at promoters suppresses antisense transcription. Nature *450*, 1031–1035.

Workman, J.L. (2006). Nucleosome displacement in transcription. Genes Dev. *20*, 2009–2017.

Yao, W., King, D.A., Beckwith, S.L., Gowans, G.J., Yen, K., Zhou, C., and Morrison, A.J. (2016). The INO80 complex requires the Arp5-Ies6 subcomplex for chromatin remodeling and metabolic regulation. Mol. Cell. Biol. *36*, 979–991.

Yen, K., Vinayachandran, V., Batta, K., Koerber, R.T., and Pugh, B.F. (2012). Genome-wide nucleosome specificity and directionality of chromatin remodelers. Cell *149*, 1461–1473.

Yuan, G.-C., Liu, Y.-J., Dion, M.F., Slack, M.D., Wu, L.F., Altschuler, S.J., and Rando, O.J. (2005). Genome-scale identification of nucleosome positions in S. cerevisiae. Science *309*, 626–630.

Zhang, L., Ma, H., and Pugh, B.F. (2011a). Stable and dynamic nucleosome states during a meiotic developmental process. Genome Res. *21*, 875–884.

Zhang, Z., Wippo, C.J., Wal, M., Ward, E., Korber, P., and Pugh, B.F. (2011b). A packing mechanism for nucleosome organization reconstituted across a eukaryotic genome. Science *332*, 977–980.

STAR★METHODS

KEY RESOURCES TABLE

REAGENT or RESOURCE	SOURCE	IDENTIFIER
Chemicals, Peptides, and Recombinant Proteins		
Alpha factor Zymo research	Y1001 Tn5 transposase	A gift from I. Amit, Weizmann Institute of Science
Auxin (3-indolo acetic acid)	Sigma-Aldrich	I2886
Proteinase K	Epicenter	MPRK092
MNase (Micrococcal nuclease)	Worthington	LS004798
SPRI beads (Agencourt AMPure XP)	Agencourt	BC-A63881
SmartScribe enzyme (SMARTScribe Reverse Transcriptase)	Clontech	639536
oligo(dt)25 beads (Dynabeads mRNA DIRECT Purification Kit)	Life technologies	61005
KAPA HiFi HotStart ReadyMix	Kapa Biosystems	ROCHE-07958927001
4tu (4-Thiouracil)	Sigma-Aldrich	440736
ZYMOLYASE	MP biomedicals	MP-08320921
Deposited Data		
Raw and analyzed data	This paper	GEO:GSE118214
GRF binding data	(Gutin et al., 2018)	GEO:GSE108948
Experimental Models: Organisms/Strains		
S. cerevisiae: BY4742, genetic background S288C, paternal strain: BY4742, MATα; his3Δ 1; leu2Δ 0; lys2Δ 0; ura3Δ 0	Euroscarf	BY4742(Y10000)
S. cerevisiae: Delta-SWR1-Nat, genetic background S288C, paternal strain: BY4742, his3Δ1 leu2Δ0 lys2Δ0 ura3Δ0 swr1Δ0::natMX6	This paper	NF104
S. cerevisiae: Delta-CHD1-Nat, genetic background S288C, paternal strain: BY4742, his3Δ1 leu2Δ0 lys2Δ0 ura3Δ0 chd1Δ0::natMX6	This paper	NF105
S. cerevisiae: Delta-ISW1-Nat, genetic background S288C, paternal strain: BY4742, his3Δ1 leu2Δ0 lys2Δ0 ura3Δ0 isw1Δ0::natMX6	This paper	NF106
S. cerevisiae: Delta-ISW2-Nat, genetic background S288C, paternal strain: BY4742, his3Δ1 leu2Δ0 lys2Δ0 ura3Δ0 isw2Δ0::natMX6	This paper	NF173
S. cerevisiae:U2721, genetic background:DF5, MATa, his3-Δ200, leu2-3,2-112, lys2-801, trp1-1(am), URA3::TIR-9Myc	Morawska and Ulrich, 2013	N/A
S. cerevisiae: CHD1-IAA*-FLAG, genetic background:DF5, paternal strain: U2721, his3-Δ200, leu2-3,2-112, lys2-801, trp1-1(am), URA3::TIR-9Myc, CHD1-44AID9Flag::hphNT	This paper	NF188
S. cerevisiae: INO80-IAA*-FLAG, genetic background:DF5, paternal strain: U2721, his3-Δ200, leu2-3,2-112, lys2-801, trp1-1(am), URA3::TIR-9Myc, INO80-44AID9Flag::hphNT	This paper	NF191
S. cerevisiae: SWR1-IAA*-FLAG, genetic background:DF5, paternal strain: U2721, his3-Δ200, leu2-3,2-112, lys2-801, trp1-1(am), URA3::TIR-9Myc, SWR1-44AID9Flag::hphNT	This paper	NF193
S. cerevisiae: SNF2-IAA*-FLAG, genetic background:DF5, paternal strain: U2721, his3-Δ200, leu2-3,2-112, lys2-801, trp1-1(am), URA3::TIR-9Myc, SNF2-44AID9Flag::hphNT	This paper	NF196
S. cerevisiae: STH1-IAA*-FLAG, genetic background:DF5, paternal strain: U2721, his3-Δ200, leu2-3,2-112, lys2-801, trp1-1(am), URA3::TIR-9Myc, STH1-44AID9Flag::hphNT	This paper	NF198
S. cerevisiae: FUN30-IAA*-FLAG, genetic background:DF5, paternal strain: U2721, his3-Δ200, leu2-3,2-112, lys2-801, trp1-1(am), URA3::TIR-9Myc, FUN30-44AID9Flag::hphNT	This paper	NF200

(*Continued on next page*)

Continued

REAGENT or RESOURCE	SOURCE	IDENTIFIER
S. cerevisiae: ISW1-IAA*-FLAG, genetic background:DF5, paternal strain: U2721, his3-Δ200, leu2-3,2-112, lys2-801, trp1-1(am), URA3::TIR-9Myc, ISW1-44AID9Flag::hphNT	This paper	NF202
S. cerevisiae: ISW2-IAA*-FLAG, genetic background:DF5, paternal strain: U2721, his3-Δ200, leu2-3,2-112, lys2-801, trp1-1(am), URA3::TIR-9Myc, ISW2-44AID9Flag::hphNT	This paper	NF204
S. cerevisiae: ΔBAR1, genetic background:DF5, paternal strain: U2721, his3-Δ200, leu2-3,2-112, lys2-801, trp1-1(am), URA3::TIR-9Myc,bar1::kanmx	This paper	NF205
S. cerevisiae: STH1-IAA*-FLAG,ΔBAR1, genetic background:DF5, paternal strain: BAR1::G418, his3-Δ200, leu2-3,2-112, lys2-801, trp1-1(am), URA3::TIR-9Myc, STH1-44AID9Flag::hphNT,bar1::kanmx	This paper	NF211
K. lactis (ASM251v)	A gift from Y. Tzfati, The Hebrew University of Jerusalem	N/A
Oligonucleotides		
CHD1-deg-F: GATGGCAATGTACGACAAGATAACAGAGTC TCAAAAGAAGcgtacgctgcaggtcgac	This paper	N/A
CHD1-deg-R: GGGGAAGGAACAATGGAAAATGTGGTGAA GAAAAATTGTTatcgatgaattcgagctcg	This paper	N/A
INO80-deg-F: AAGTCAAGATGGAATTAAGGAAGCGGC AAGTGCATTGGCAcgtacgctgcaggtcgac	This paper	N/A
INO80-deg-R: AACTCCGCTTAATGTAAATAACACAATATGAA TACCTTTTatcgatgaattcgagctcg	This paper	N/A
SWR1-deg-F: CGAGTACATGATCAGGTTTATTGCCAACGGTTA TTATTATcgtacgctgcaggtcgac	This paper	N/A
SWR1-deg-R: TGGACAACTAAGGCAGCGGTGAAGAGTAGAAC CTGGTCCTatcgatgaattcgagctcg	This paper	N/A
SNF2-deg-F: CACAGATGAAGCGGACTCGAGCATGACAG AAGCGAGTGTAcgtacgctgcaggtcgac	This paper	N/A
SNF2-deg-R: CGTATAAACGAATAAGTACTTATATTGCTT TAGGAAGGTAatcgatgaattcgagctcg	This paper	N/A
STH1-deg-F: AAATGAGTTTACTGATGAATGGTTCAAGGA ACACTCTTCGcgtacgctgcaggtcgac	This paper	N/A
STH1-deg-R: ATATAGTCGTAAAAAAAAAAAACATGTGGTGATGAA AACGatcgatgaattcgagctcg	This paper	N/A
FUN30-deg-F: AATTTATGATGAAAACTCGAAACCGAAGGGAACC AAAGAAcgtacgctgcaggtcgac	This paper	N/A
FUN30-deg-R: TCTGCTTATCTATTTACTTTTTTACTA TATTTTTATTTATatcgatgaattcgagctcg	This paper	N/A
ISW1-deg-F: GTTGGTAGCAGAGAAAATTCCGGAAAAC GAAACCACTCATcgtacgctgcaggtcgac	This paper	N/A
ISW1-deg-R: AGGATATATTAAAAAAAATCGAAATATAAAA AAAGAAGGTatcgatgaattcgagctcg	This paper	N/A
ISW2-deg-F: CGATCATGTTGATAAAAGAACCAAAATTGATCAAGAA GCAcgtacgctgcaggtcgac	This paper	N/A
ISW2-deg-R: ATATCTCTCACGTCACTTATTTTAATGCAC AATACATGATatcgatgaattcgagctcg	This paper	N/A
Illumina FC-121-1030: TCGTCGGCAGCGTCAGATGTGTA TAAGAGACAG	Ilumina	FC-121-1030
Tn5-ME-rev: 5′-[phospho]CTGTCTCTTATACACATCT	(Picelli et al., 2014a)	N/A
Tn5_A_Rd1: TCGTCGGCAGCGTCAGATGTGTATAAG AGACAG	(Picelli et al., 2014a)	N/A

(*Continued on next page*)

Continued

REAGENT or RESOURCE	SOURCE	IDENTIFIER
TSO: GACGTGTGCTCTTCCGATCTrGrG+G)	(Picelli et al., 2014b)	N/A
oligo-dT RT primers CGATTGAGGCCGGTAATACGACTCACTAT AGGGGCGACGTGTGCTCTTCCGATCTnnnnnnnNNNNNNNN TTTTTTTTTTTTTTTTTTN	A gift from I. Amit, Weizmann Institute of Science	N/A
2P_barcode: CAAGCAGAAGACGGCATACGAGATNNNNNNNNG TGACTGGAGTTCAGACGTGTGCTCTTCCGATCT	http://www.lncrna-test.caltech.edu/protocols/SPRITE_Protocol_DNA_January_2018.pdf	N/A
Software and Algorithms		
Bowtie2	(Langmead and Salzberg 2012)	http://bowtie-bio.sourceforge.net/bowtie2/index.shtml
Samtools	(Li et al., 2009)	http://samtools.sourceforge.net/

CONTACT FOR REAGENT AND RESOURCE SHARING

Further information and requests for resources and reagents should be directed to and will be fulfilled by the Lead Contact, Nir Friedman (nir.friedman@mail.huji.ac.il).

EXPERIMENTAL MODEL AND SUBJECT DETAILS

Saccharomyces cerevisiae yeast strains used in this study are listed in Key Resources Table. Auxin inducible degradation domain was PCR-amplified from plasmid pHyg-AID*-6FLAG (primers are listed in Key Resources Table) and introduced into TIR1 expressing cells immediately before the target gene stop codon (plasmid pHyg-AID*-6FLAG and TIR1 cells are a gift from Ulrich lab (Morawska and Ulrich, 2013)).

In all experiments, yeast cells were grown in YPD at 24°C with constant shaking to OD 0.3-0.6. When indicated, Auxin (3-indolo acetic acid, Sigma) was added at final concentration of 0.5 mM. 250 mM Auxin stock was prepared in EtOH. Ethanol was also added to control samples as mock treatment. To induce stress, KCl was added at a final concentration of 0.4 M. For cell cycle arrest, alpha factor was added at a final concentration of 2.5×10^{-7} M to Δbar1 cells.

METHOD DETAILS

MNase digestion and DNA Sequencing

MNase digestion was carried out using as previously described (Shivaswamy et al., 2008; Weiner et al., 2010). Briefly, cells were fixed in 1% formaldehyde for 15 minutes, and then formaldehyde was quenched by glycine addition at a final concentration of 125 mM. Cells were washed and their pellet was kept in −80°C and then resuspended in Zymolyase buffer and treated with Zymolyase (6U/od) for 25 minutes at 30°C to generate spheroplasts. Spheroplasts were washed, resuspended in NP buffer and treated with MNase (Micrococcal nuclease, Worthington) to generate 80% mono-nucleosomes (1 unit for 2.5 OD initial culture, 37°C, 20 minutes). Reaction was stopped by adding 0.5% SDS and 25 mM EDTA.

MNase digested chromatin was reverse cross linked, and MNase sequencing libraries were prepared as previously described (Blecher-Gonen et al., 2013) and sequenced using Illumina technology.

RNA purification and 3′-Library preparation

Cell pellet was flash frozen in liquid nitrogen and kept in -80°C except for the spike-in experiment where both Sth1-degron and Kluyveromyces lactis cells were fixed in formaldehyde as described above, resuspended in water and cell concentration was determined under the microscope using a hemocytometer and 5% lactis were added to each sample.

RNA purification was performed as previously described (Dye et al., 2005). Briefly, RNA was released from the cells by digestion with Proteinase K (Epicenter) in the presence of 1% SDS at 70°C. Cell debris and proteins were precipitated by centrifugation in the presence of potassium acetate. RNA was then purified from the supernatant using nucleic acid binding plates (96-well, 800 μl UNIFILTER Microplate, GE Healthcare) and was stored with RNase-inhibitor at −80°C.

Total RNA (0.5 ug RNA per library, but not less than 20 ng per sample) was incubated with oligo-dT RT primers with 7bp barcode and 8bp UMI (Unique Molecular Identifier) at 72°C for 3 minutes and transferred immediately to ice. RT reaction was performed with SmartScribe enzyme (SMARTScribe Reverse Transcriptase, Clontech) at 42°C for one hour followed by incubation at 70°C for 15 minutes. Barcoded samples were then pooled and purified using SPRI beads X1.2 (Agencourt AMPure XP, Beckman

Coulter). DNA-RNA hybrids were tagmented using Tn5 transposase (loaded with oligos Tn5MEDS-A, Key Resources Table) and 0.2% SDS was added to strip off the Tn5 from the DNA (Picelli et al., 2014a), followed by a SPRI X2 cleanup. NGS sequences were added to the tagmented DNA by PCR (KAPA HiFi HotStart ReadyMix, Kapa Biosystems, 12 cycles). And the DNA was purified using 0.8x SPRI beads. Library was sequenced using Illumina NextSeq-500 sequencer with an average of 700,000 aligned reads per sample.

Metabolic labeling and SLAM-Seq

Metabolic labeling of newly synthesized RNA molecules was done as previously described (Voichek et al., 2016). Briefly, 4-thiouracil (4tU) (Sigma) was dissolved in NaOH and added to cells at final concentration of 5 mM 4tU. To avoid pH change as a result of NaOH addition, MES buffer was added to the media. At different time points after auxin addition, 4tU was added to cells for ten minutes, cells were fixed in methanol and RNA purification was done as described above. Total RNA was subjected to thiol(SH)-linked alkylation by iodoacetamide (Sigma, 10 mM) at 50°C for 15 minutes (Herzog et al., 2017), the reaction was stopped by 20 mM DTT and RNA was purified using nucleic acid binding plates (96-well, 800 μl UNIFILTER Microplate, GE Healthcare). 3′-library was prepared and sequenced as above.

5′-Library preparation

Cell pellet was resuspended in proteinase K solution (10 mM Tris pH 8.0, 5 mM EDTA pH 8.0, 150 mM NaCl, 1% sodium dodecyl sulfate (SDS), 0.4 mg/mL proteinase K (Epicenter)) in the presence of oligo(dt)25 beads (Dynabeads® mRNA DIRECT Purification Kit, Life technologies) that were pre-washed with Proteinase K buffer (Epicenter MPRK092). RNA was released from the cells at 70°C for 15 minutes, followed by 5 minutes incubation at RT to allow mRNA hybridization to polyT beads. Beads-mRNA complexes were washed according to the manufacturer protocol except that buffer B was prepared without EDTA. Reverse transcription was performed on the beads with SmartScribe enzyme in the presence of 1 μM of Template Switching Oligo (Picelli et al., 2014a) (TSO, Key Resources Table). cDNA was washed on beads and second strand synthesis was performed using KAPA HiFi HotStart ReadyMix (Kapa Biosystems) and barcoded oligo (2P_barcode, Key Resources Table). Pooled samples were then tagmented as above (except that it was performed on the beads). Supernatant (containing the 5′-fragments of the mRNA) was transferred to a new tube followed by a SPRI X2 clean up. NGS sequences were added to the tagmented DNA by PCR (KAPA HiFi HotStart ReadyMix, Kapa Biosystems, 12 cycles) and the DNA was purified using 0.8x SPRI beads. Library was sequenced using Illumina NextSeq-500 sequencer with an average of 10 million aligned reads per sample.

QUANTIFICATION AND STATISTICAL ANALYSIS

Nucleosome mapping and features

Single-end or paired-end reads were mapped to the yeast (sacCer3) genomes using bowtie2 default parameters. Fragments longer than 200 bp were filtered out. For paired-end data, we used fragment centers for the rest of the analysis. For single end data, we approximated fragment center to be 75 bp downstream to the read start position when it is aligned to the "+" strand, or upstream to the read start position when it is aligned to the "-" strand, and used it for the rest of the analysis.

We calculated coverage over the genome from fragment centers using MATLAB "ksdensity" function with width 30. To call nucleosome peaks, we first identified local maxima in the coverage of each experiment and selected the ones with the highest coverage as the centers of nucleosomes. In time course experiments, the movement of each nucleosome was identified according to the "closest" nucleosome position in a previous time point. We annotated nucleosome positions along the gene (−1,+1,+2,…,+N) based on TSS mapping data (Weiner et al., 2015). Nucleosome +1 was defined as the first nucleosome after the TSS position. −1 was defined the nucleosome upstream to +1. NFR width was defined as the distance between centers of +1 and −1 peaks.

To define nucleosome fuzziness we checked the distribution of the read centers forming the nucleosome peak, in 150 bp window around the nucleosome peak. We calculated the distance between the position of 20% and 80% quantiles of the read centers in this window.

For metagene plots, genes were oriented according to the gene directionality and aligned around the TSS or around nucleosome peak as described. Finally, the median coverage in the aligned regions or the sum of read centers was plotted.

3′ RNA data - Sequence Analysis

For 3′ RNA data analysis, reads were mapped to the *S. cerevisiae* (sacCer3) genome using bowtie2 with default parameters. We used UMI to filter duplicate reads. We then classified reads to genes TSS region (350 bp upstream to 200 bp downstream of the TTS). We counted the reads that were classified for each gene in each sample. We normalized the reads number per gene in every sample by the overall number of reads that were mapped and classified to TSS in that sample and multiplied by 10^6 (ppm normalization).

For the analysis of the spike-in experiments data, we used bowtie2 to align the sequenced library twice: to *S. cerevisiae* (sacCer) and to *K. lactis* (ASM251v). We discarded reads that mapped to both strains. For each sample we calculated the ratio between the number of reads that were mapped to *S. cerevisiae* genome and the number of reads that were mapped to *K. lactis* genome. We used the average between ratios calculated in 2 repeat samples as a spike-in normalization factor.

Next, we used the normalization factor to normalize the data - we merged repeats, classified reads to TTS regions for each sample, and normalized reads number for each sample as described above. We multiplied the normalized reads count by its relevant spike-in normalization factor.

5′ RNA data analysis

For 5′ RNA data analysis, reads were mapped to the *S. cerevisiae* (sacCer3) genome using bowtie2 with local mode. G tracks were removed from the reads starts before the alignment. We used spike-in normalization factor that was previously calculated for 0h, 0.5h, and 2h for the normalization of our 5′ data. We used regression to estimate a spike-in normalization factor for 1h sample. To normalized the 5′ data, we divided each sample by the number of reads that were mapped and multiplied by 10^6 (ppm normalization). We multiply the reads number through the genome by the relevant spike-in normalization factor.

To define accessibility of a TSS position, we used the MNase coverage in that position normalized by the maximum coverage in 200 bp window around it. The accessibility is defined as (1-normalized coverage). The set of genes with a high fraction of occluded TSSs was defined as follows: First, we defined a set of expressed TSS positions (log2(normalized 5′ level +1) > 2) with low accessibility level (< 0.15). Then, we found a set of genes with TSS annotation close to the TSS positions in this set (< 200 bp). Finally, for each gene we calculate the fraction of TSS positions (in window of −200 to +100 around nucleosome +1) that are not accessible. we chose only genes with more than 50% of the TSS positions are not accessible in steady state.

DATA AND SOFTWARE AVAILABILITY

The accession number for the sequence data reported in this paper is GEO: GSE118214.

Cell Reports, Volume *26*

Supplemental Information

Dynamics of Chromatin and Transcription during Transient Depletion of the RSC Chromatin Remodeling Complex

Avital Klein-Brill, Daphna Joseph-Strauss, Alon Appleboim, and Nir Friedman

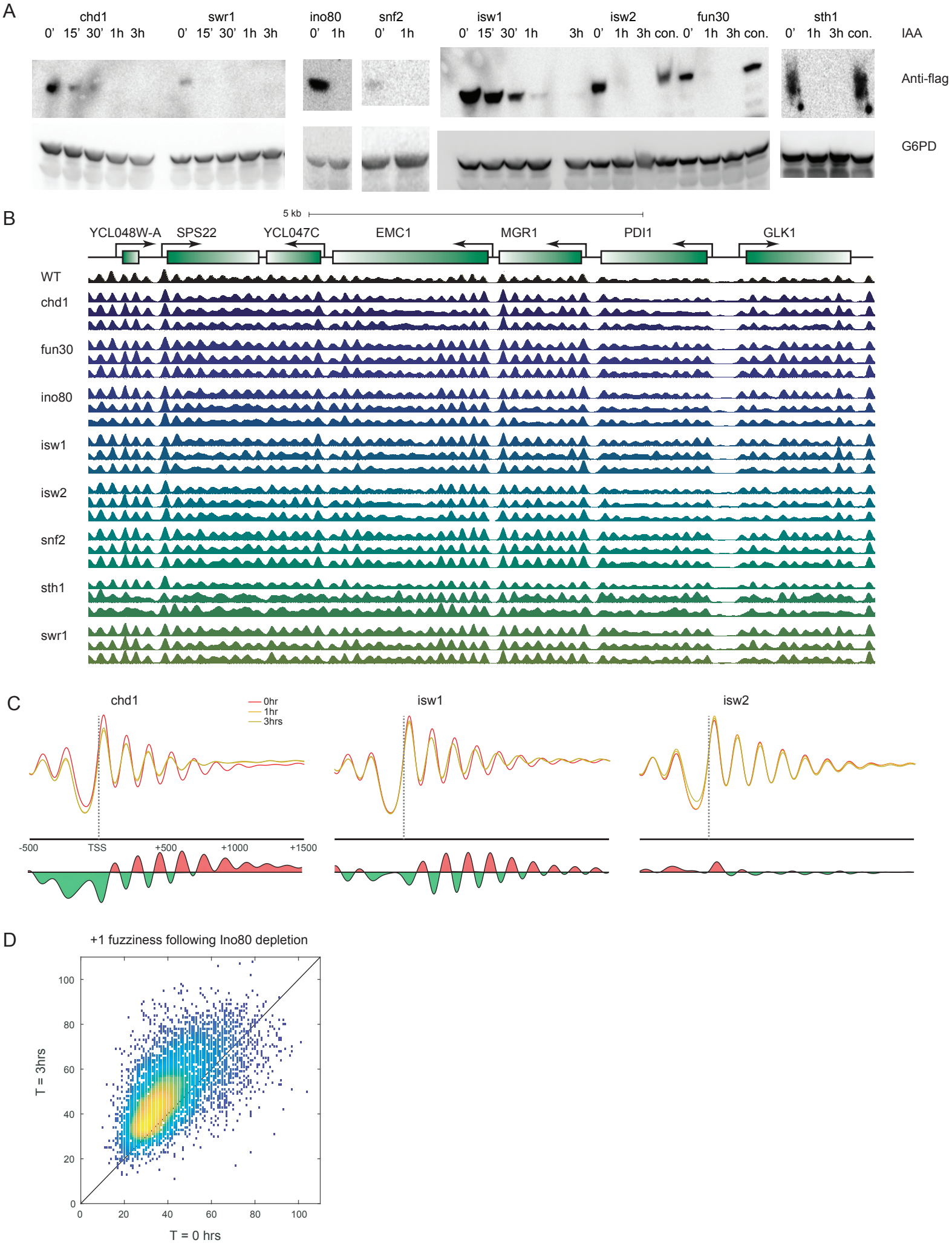
A
chd1
0' 15' 30' 1h 3h
swr1
0' 15' 30' 1h 3h
ino80
0' 1h
snf2
0' 1h
isw1
0' 15' 30' 1h
isw2
3h 0' 1h 3h con.
fun30
0' 1h 3h con.
sth1
0' 1h 3h con.
IAA
Anti-flag
G6PD
B
5 kb
YCL048W-A
SPS22
YCL047C
EMC1
MGR1
PDI1
GLK1
WT
chd1
fun30
ino80
isw1
isw2
snf2
sth1
swr1
C
chd1
0hr
1hr
3hrs
isw1
isw2
-500
TSS
+500
+1000
+1500
D
+1 fuzziness following Ino80 depletion
T = 3hrs
T = 0 hrs
0
20
40
60
80
100

Supplementary Figure 1: Induced knockdown screen of ATP-dependent chromatin remodelers, related to Figure 1

A. Western blot analysis of all 8 ATPAse subunits show drastic reduction of flag-degron-tagged proteins after introduction of auxin.

B. Nucleosome positions in all 8 AID strains before and after induction of auxin in a 10Kb genomic region.

C. Average MNase coverage positioned relative to the TSS, (as in Figure 1C,extended to gene body)

D. Fuzziness of nucleosome +1 of all genes before and 3 hours after auxin induction in Ino80 AID strain. Fuzzyness is defined as the distance between the 20%th and 80%th centers of reads assigned to the same nucleosome peak.

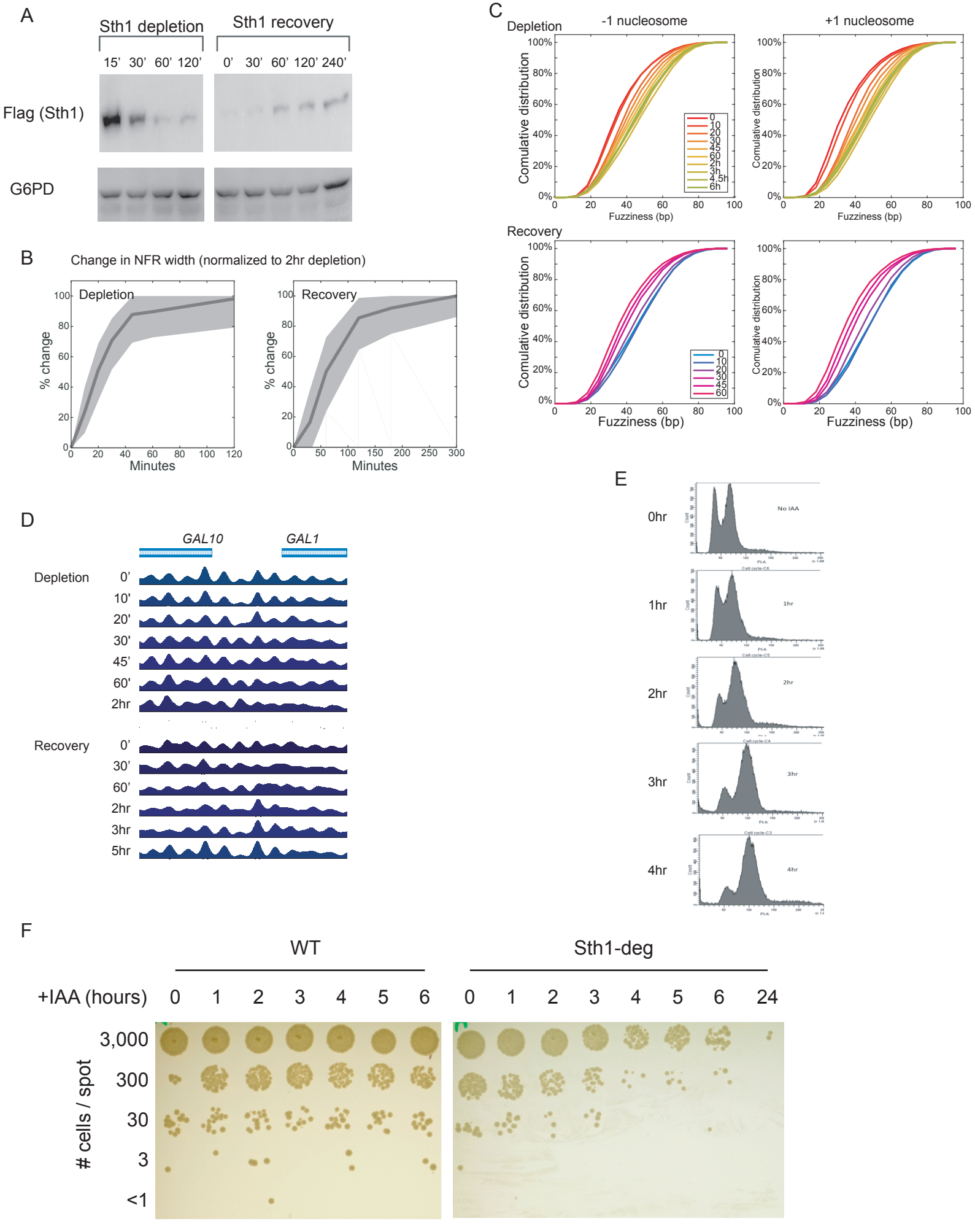
A
Sth1 depletion
Sth1 recovery
15' 30' 60' 120'
0' 30' 60' 120' 240'
Flag (Sth1)
G6PD
B
Change in NFR width (normalized to 2hr depletion)
Depletion
Recovery
% change
Minutes
C
Depletion
-1 nucleosome
+1 nucleosome
Recovery
Comulative distribution
Fuzziness (bp)
0
10
20
30
45
60
2h
3h
4.5h
6h
D
GAL10
GAL1
Depletion
0'
10'
20'
30'
45'
60'
2hr
Recovery
0'
30'
60'
2hr
3hr
5hr
E
0hr
1hr
2hr
3hr
4hr
No IAA
F
WT
Sth1-deg
+IAA (hours)
0 1 2 3 4 5 6 0 1 2 3 4 5 6 24
cells / spot
3,000
300
30
3
<1

Supplementary Figure 2: Dynamics of Sth1 depletion and recovery show massive yet reversible disruptions in chromatin organization, related to Figure 2

A. Western blot analysis of Degron-tagged-Sth1 during addition (Sth1-depletion) and removal (Sth1-recovery) of auxin shows drastic reduction in protein levels after introduction of auxin and partial recovery of the protein following removal of auxin from the media.

B. Percent of change in NFR width at each time point out of the maximal change following Sth1 depletion (left) and recovery (right). Lines are medians, shaded areas include 20-80% of genes

C. Cumulative distribution of the fuzziness of -1 (left) and +1 (right) nucleosomes following Sth1 depletion and recovery.

D. Coverage following Sth1 depletion and recovery in Gal1 and Gal10 promoter area.

E. Cellular DNA content measured by FACS following RSC depletion. Cells are arrested following Sth1 depletion.

F. Survival test of WT and degron-Sth1 strains following auxin induction. Cells were incubated in the presence of auxin for the indicated times, serial diluted and spotted on YPD plates. Plates were incubated for 2-3 days in 30^0C.

A Depletion

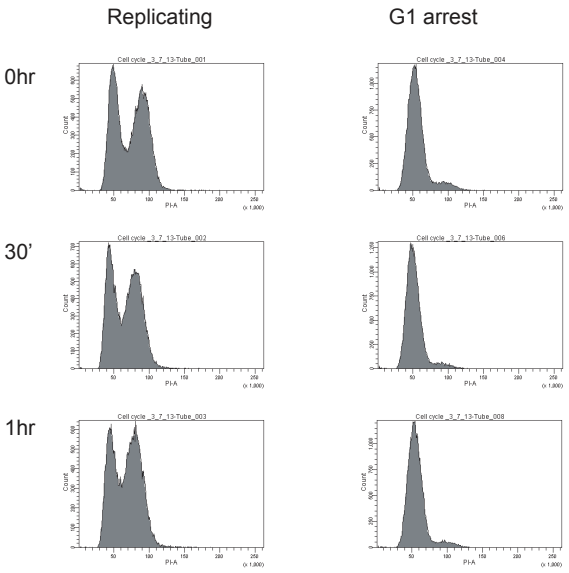

B Recovery

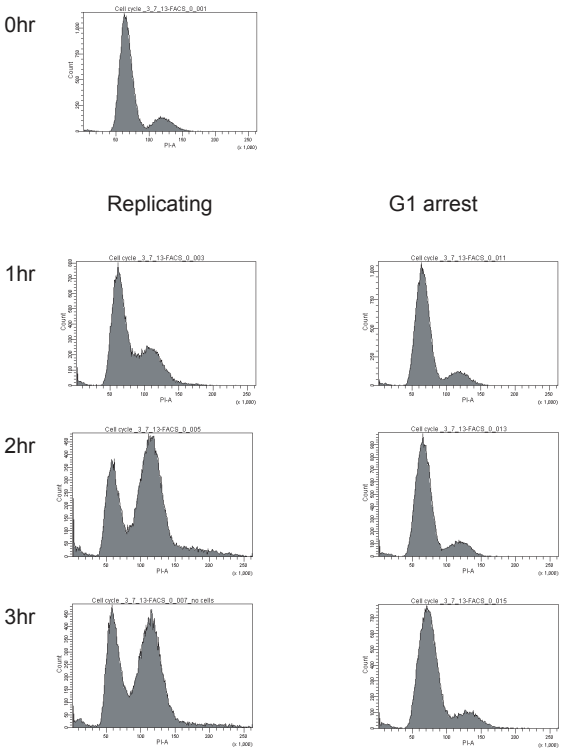

Supplementary Figure 3: Sth1-dependent NFR clearing is replication independent, related to Figure 3

A. Cellular DNA content measured by FACS following RSC depletion in G1 arrested cells and in replicating cells.

B. Cellular DNA content measured by FACS following RSC recovery in G1 arrested cells and in replicating cells.

A Gene expression levels compared to pre IAA addition expression (log2)

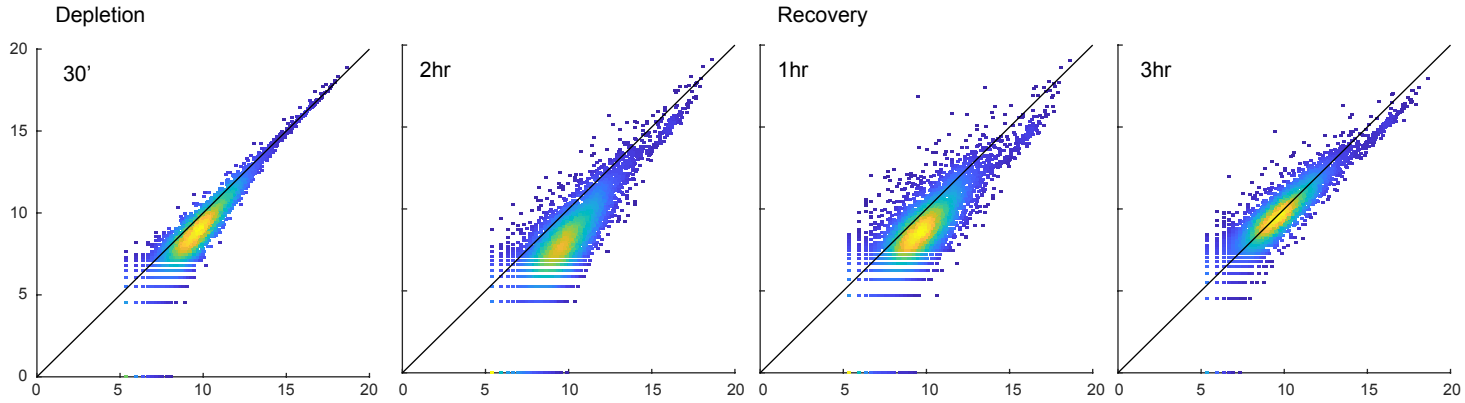

B

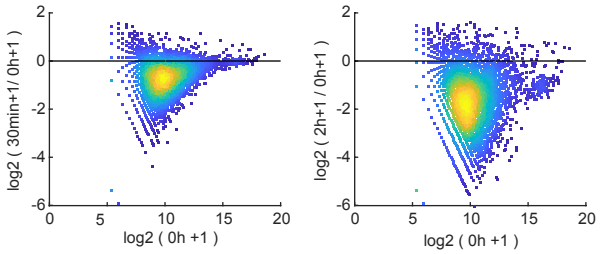

C SLAM-seq conversion rates (total mRNA)

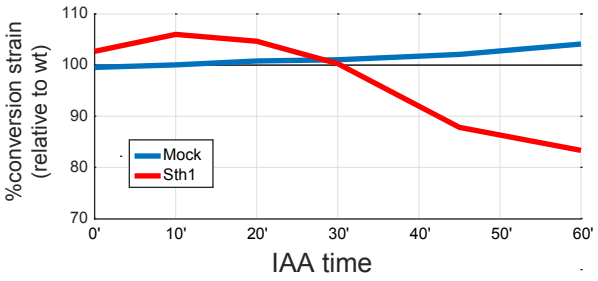

SLAM-seq conversion rates (individual genes)

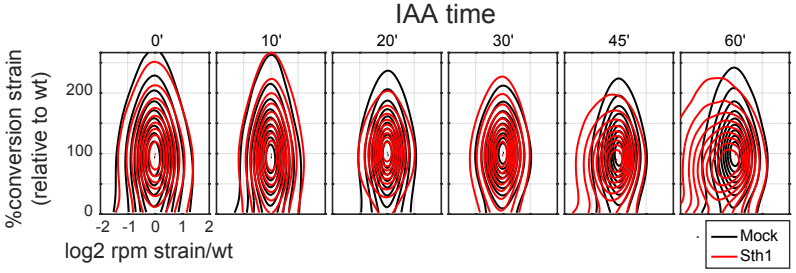

D

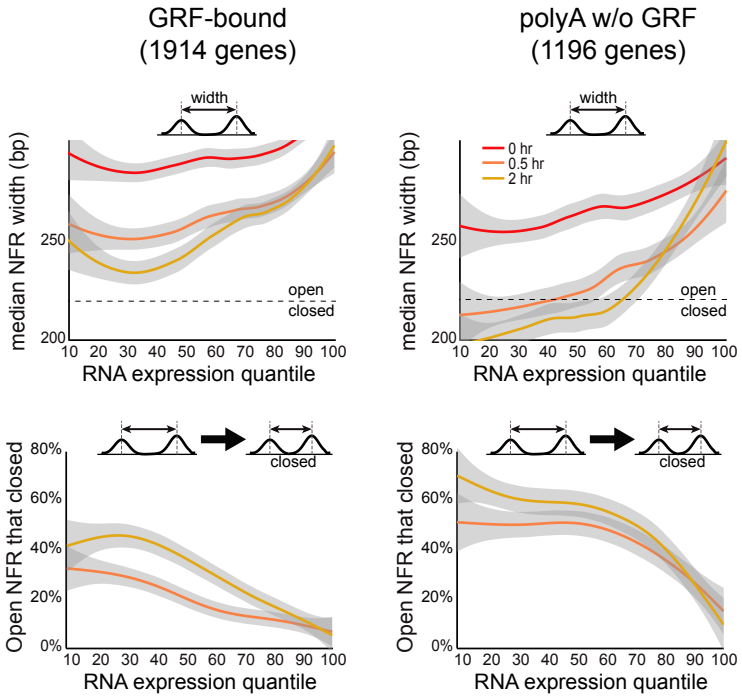

Supplementary Figure 4: RSC maintains open NFRs in lowly-expressed genes but not necessary for acute transcriptional response, related to Figure 4

A. RNA level during Sth1 depletion and recovery vs. RNA level before auxin was added . RNA level was normalized with *K. lactis* spike-in.

B. RNA fold change during Sth1 depletion and recovery vs. RNA level before auxin was added. RNA level was normalized with *K. lactis* spike-in.

C. Changes in rates of RNA synthesis during Sth1 depletion using SLAM-seq (Methods). Changes in percent new RNA (reads w/ converted base) for Sth1 depletion and mock strain in the total mRNA population (left) and distribution of changes for individual genes (right). All changes are shown relative to WT strain processed in parallel.

D. Same as Figure 4C, broken for the two groups of genes shown in Figure 2E.

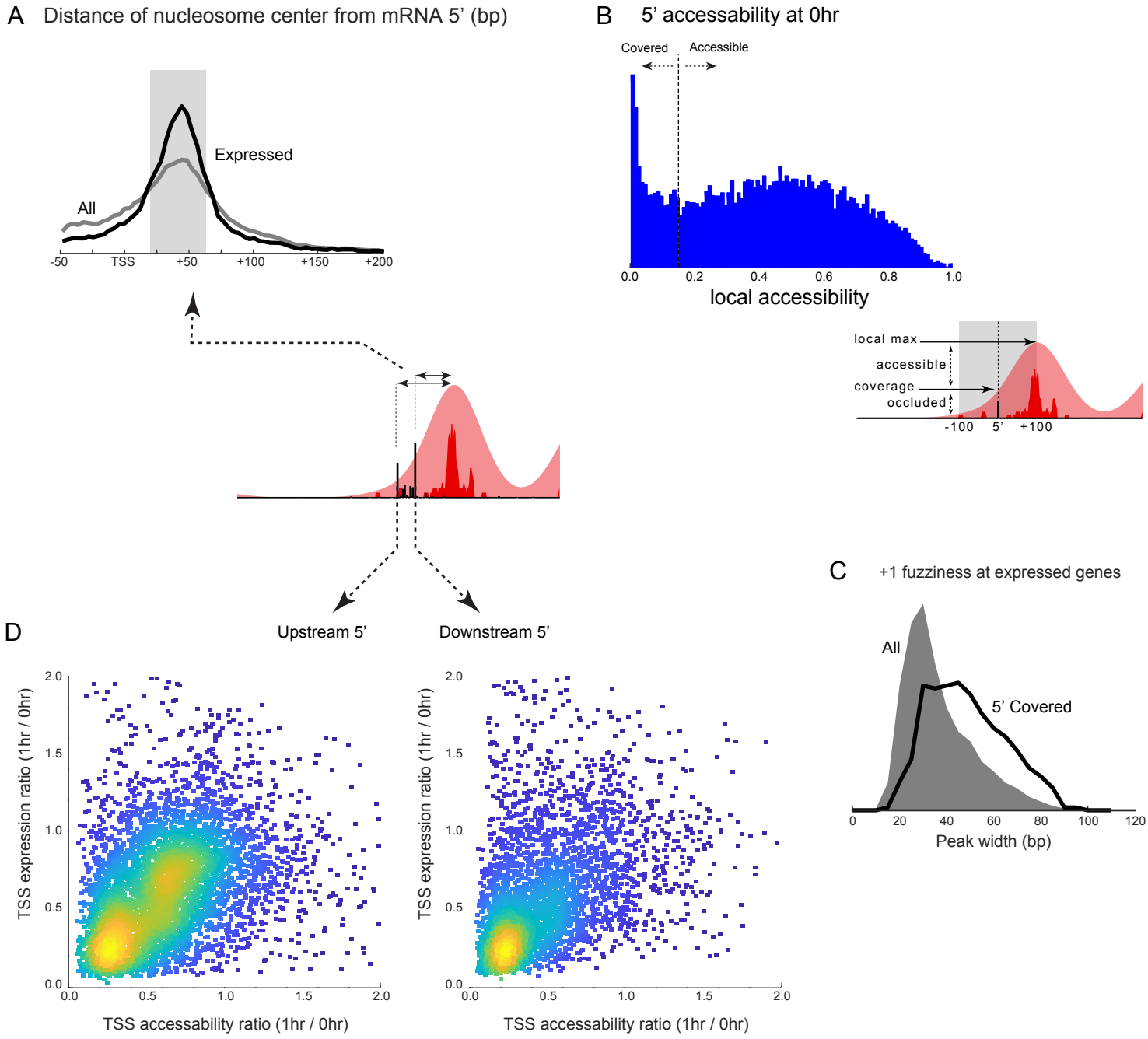
A
Distance of nucleosome center from mRNA 5' (bp)
Expressed
All
-50
TSS
+50
+100
+150
+200
B
5' accessability at 0hr
Covered
Accessible
0.0
0.2
0.4
0.6
0.8
1.0
local accessibility
local max
accessible
coverage
occluded
-100
5'
+100
Upstream 5'
Downstream 5'
C
+1 fuzziness at expressed genes
All
5' Covered
0
20
40
60
80
100
120
Peak width (bp)
D
TSS expression ratio (1hr / 0hr)
TSS accessability ratio (1hr / 0hr)
0.0
0.5
1.0
1.5
2.0

Supplementary Figure 5: Changes in +1 nucleosome position are reflected in TSS usage, related to Figure 5

A. Distribution of the distance of nucleosome center from mRNA 5' position for all genes (grey line) and a subset of expressed gene (black line).

B. Histogram of TSS accessibility measure used to define transcription start sites that are covered by nucleosome.

C. Fuzziness of +1 nucleosome for genes whose 5' locations are covered.

D: As in Figure 5E for two subsets of 5' positions, defined by their location relative to other TSSs of the same gene. Left panel for downstream and right panel for upstream TSS.

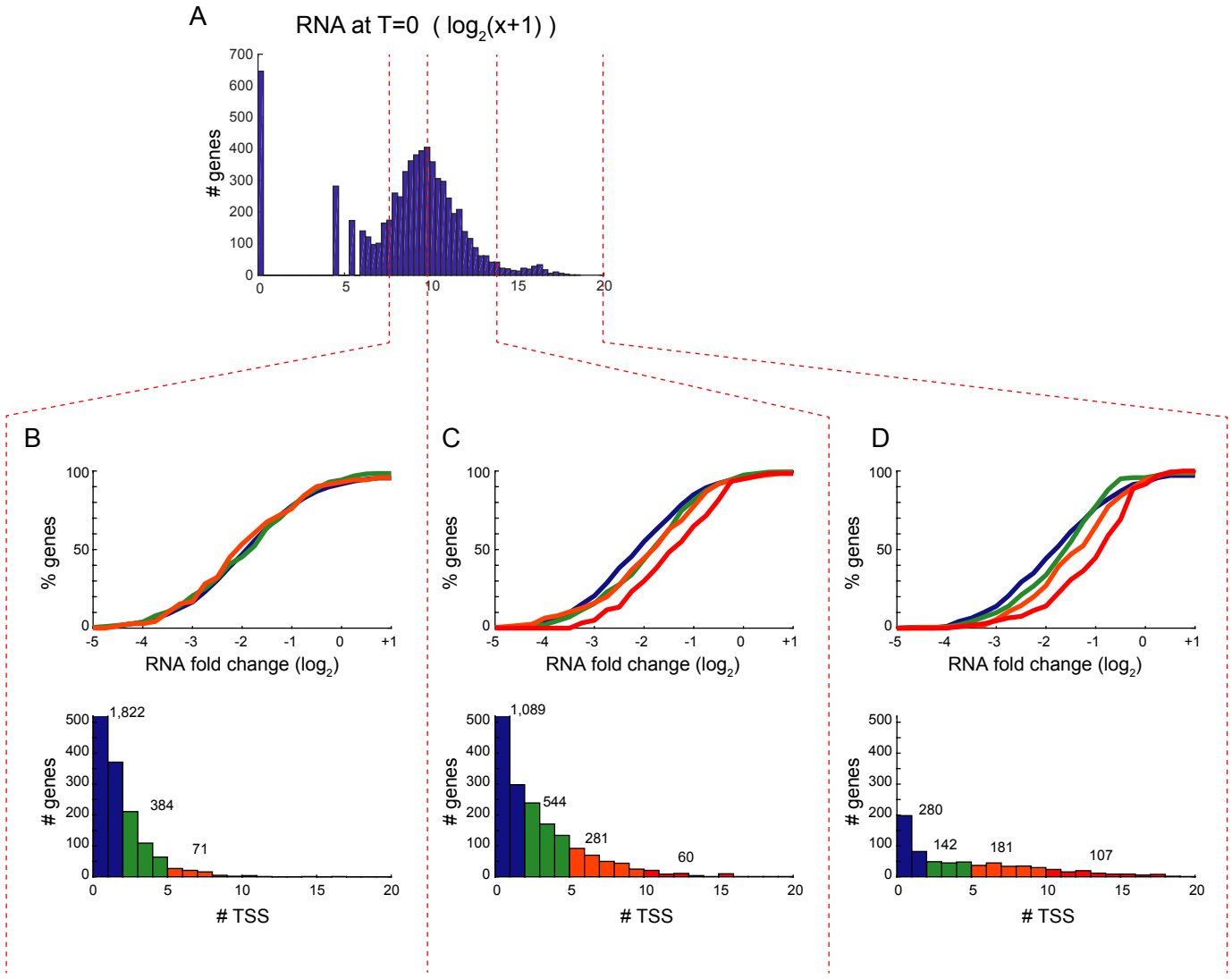
A
RNA at T=0 (log2(x+1))
genes
B
C
D
% genes
RNA fold change (log2)
genes
TSS
1,822
384
71
1,089
544
281
60
280
142
181
107

Supplementary Figure 6: Changes in 5' TSS accessibility are indicative of changes in gene expression levels, related to Figure 6

A. Histogram of expression levels (x-axis) of genes, based on 3' RNA-seq before depletion. Three ranges of expression are marked (low, mid, high expressed).

B-D. For each range of expression shown is the cumulative distribution of fold change in RNA following depletion (log base 2) broken down to four classes of genes (top). Also shown is the histogram of number of genes in the range broken down according the number of TSS positions for the gene before depletion.